Journal of Coordination Chemistry, 2014
Vol. 67, Nos. 23–24, 3734–3768, http://dx.doi.org/10.1080/00958972.2014.937340

Taylor & Francis
Taylor & Francis Group

Review: Natural oxalates and their analogous synthetic complexes

ENRIQUE J. BARAN*

Facultad de Ciencias Exactas, Centro de Química Inorgánica (CEQUINOR/CONICET,UNLP), Universidad Nacional de La Plata, La Plata, Argentina

(*Received 19 March 2014; accepted 18 May 2014*)

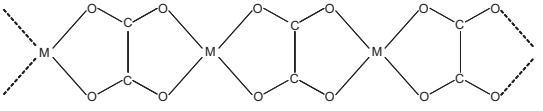

M = Mg(II), Mn(II), Fe(II), Co(II), Ni(II), Zn(II)

Metal oxalates, commonly classified as organic minerals, are widely distributed in Nature, occurring in mineral deposits or as biominerals in plants, fungi, and lichens or in the form of deposits, of different kinds, in animal tissues. Eighteen natural species of this type have so far been reported and investigated. In the first part of this review we give an overview on the general characteristics of these minerals, including also some comments on their environmental effects. The central part of the review is devoted to the discussion of synthetic oxalates, analogous to the natural species, including the usual procedures employed for their synthesis and the thorough analysis of their crystallographic and structural peculiarities. The thermal, spectroscopic, and magnetic properties of these complexes are also discussed in detail. Some comparisons with related coordination compounds are also made along the text.

Keywords: Oxalate minerals; Synthetic analogous complexes; Synthesis; Structural properties; Thermal, spectroscopic and magnetic behavior

1. Introduction

Metallic crystalline oxalates are widely distributed in Nature and have been observed in rocks, soil, water bodies, and among a variety of living organisms, including plants and animals. They constitute a group of relatively rare and scarce minerals which are usually classified as "organic crystals" or "organic minerals" [1–3]. Some of these crystals are found in living organisms (the so-called biominerals) and are generated through some of the well-known biochemical and physiological strategies used for the formation of such deposits [2, 4, 5].

*Email: baran@quimica.unlp.edu.ar
Dedicated to my dear friend Prof. Juan Costamagna, on the occasion of his retirement.

Carboxylate minerals, i.e. oxalate, formate, and acetate minerals, constitute the largest family of organic minerals and, between them, the oxalates are the most abundant group, with 18 different species reported so far, including three recently reported sulfato–oxalato and one silico–aluminate–oxalato species as shown in table 1.

Calcium oxalate minerals (the mono-, di-, and tri-hydrates of $Ca(C_2O_4)$, are the most common family of organic minerals in natural environments, usually occurring in carbonate concretions, marine and lake sediments, hydrothermal veins, and lignite [3].

Calcium oxalates are also the most common and abundant biominerals found in the plant kingdom [3, 6–9] and widely recognized in the life sciences due of their common association with kidney stone disease (urolithiasis) [6]. The presence of other metallic oxalates is extremely rare in biological systems, although the respective copper, magnesium, and manganese complexes have been detected in some lichens, whereas natural ammonium oxalate (oxamite) has been found in guano deposits. Some other of the relatively rare natural metallic oxalates included in table 1 have been described in recent years although their origin is often not totally clear [6].

Oxalic acid, ethanedioic acid, is the simplest of the dicarboxylic acids. The acid and some of its salts have been known for more than 200 years. The form usually used in chemistry laboratories, obtained by water recrystallization, is the monoclinic dihydrate, $(COOH)_2{\cdot}2H_2O$, space group $P2_1/n$ and $Z = 2$ [10, 11]. Its protonation equilibria have often been investigated; the pK values obtained at 25 °C and at ionic strength of 0.1 M are $pK_1 = 1.04$ and $pK_2 = 3.82$ [12] indicating that oxalic acid is a strong organic acid.

The acid generates a great variety of salts and complexes with practically all known metallic oxides or bases and the oxalate anion is a well-known and widely investigated ligand in coordination chemistry [13]. It is potentially a tetradentate ligand, but it can of course also act in a mono-, bi-, or tri-dentate fashion, forming mononuclear or polynuclear metal complexes. A recent survey of more than 800 oxalate-containing complexes for which structural information is available has shown that the anion possesses 15 different coordination modes with respect to metal centers, and depending on the coordination mode,

Table 1. List of the so far known natural oxalate minerals.

Mineral name	Chemical composition
Natroxalate	$Na_2(C_2O_4)$
Whewellite	$Ca(C_2O_4){\cdot}H_2O$
Wedellite	$Ca(C_2O_4){\cdot}2H_2O$
Caoxite	$Ca(C_2O_4){\cdot}3H_2O$
Novgorodovaite	$Ca_2(C_2O_4)Cl_2{\cdot}2H_2O$
Glushinskite	$Mg(C_2O_4){\cdot}2H_2O$
Oxamite	$(NH_4)_2(C_2O_4){\cdot}H_2O$
Humboldtine	$Fe^{II}(C_2O_4){\cdot}2H_2O$
Moolooite	$Cu^{II}(C_2O_4){\cdot}nH_2O$
Lindbergite	$Mn^{II}(C_2O_4){\cdot}2H_2O$
Wheatleyite	$Na_2Cu^{II}(C_2O_4)_2{\cdot}2H_2O$
Minguzzite	$K_3Fe^{III}(C_2O_4)_3{\cdot}3H_2O$
Stepanovite	$NaMgFe^{III}(C_2O_4)_3{\cdot}8–9H_2O$
Zhemchuzhnikovite	$NaMg(Al,Fe^{III})(C_2O_4)_3{\cdot}8H_2O$
Coskrenite	$(Ce,Nd,La)_2(SO_4)_2(C_2O_4){\cdot}8H_2O$
Levinsonite	$(Y,Nd,La)_2(SO_4)_2(C_2O_4){\cdot}12H_2O$
Zugshunstite	$(Ce,Nd,La)_2Al(SO_4)_2(C_2O_4){\cdot}8H_2O$
Kyanoxalite	$Na_7[(Al_{5\text{-}6}Si_{6\text{-}7}O_{24})(C_2O_4)_{0.5\text{-}1}]{\cdot}5H_2O$

oxalate ions can form from one to eight metal–oxygen bonds [14], confirming the wide versatility of this ligand.

As increasing evidence for the presence of different metallic oxalates in different natural and biological environments has been accumulated in the last years it seems now interesting to give a brief account of these findings and also to relate them to the chemical and physicochemical characteristics of the analogous synthetic oxalate complexes to contribute to a better understanding of the characteristics of the natural compounds and to systematize in some way this peculiar field of coordination chemistry.

2. Natural metallic oxalates

2.1. *Metallic oxalates found in the mineral kingdom*

By far, the most common calcium oxalate mineral in all environments is whewellite, $Ca(C_2O_4)\cdot H_2O$, while the corresponding dihydrate, weddellite, is subordinate [15]. Even rarer is the mineral caoxite, $Ca(C_2O_4)\cdot 3H_2O$, which is found only very sporadically. From the thermodynamic point of view $Ca(C_2O_4)\cdot H_2O$ is the most stable phase [3, 6, 16, 17].

Whewellite has usually been found in three main types of deposits: near-surface/biological; diagenetic, and hydrothermal occurrences. Near-surface and biological occurrences have been reported from soils, lichens, rock patinae, oxidized ores, recent marine, and non-marine sediments, and guano. In all these cases, the association of oxalate phases with organic material providing a source of oxalate is obvious. In diagenetic environments, whewellite is closely associated with sediment sequences rich in organic matter such as coal beds and black shales, whereas in hydrothermal environments it occurs as a late-stage phase in hydrothermal veins in which well-developed druses of the mineral appear often associated with carbonates and sulfides [15].

Weddellitte was initially found in the form of millimeter-sized crystals in bottom sediments of the Weddell Sea (Antarctica) [18] and was later detected in caves from Western Australia, southern England, and different regions of the United States of America. From the chemical point of view this dihydrate must be better formulated as $Ca(C_2O_4)\cdot(2+x)H_2O$, where $0 < x \leq 0.5$, and the fractional waters of hydration are of zeolitic nature [6, 19]. Finally, caoxite which is probably of hydrothermal origin, was originally found in the Cerchiara mine near Faggiona, eastern Liguria (Italy), associated with quartz, barite, and an unidentified manganese oxide [20, 21].

The rarest of all calcium oxalate minerals so far identified is novgorodovaite, $Ca_2(C_2O_4)Cl_2\cdot 2H_2O$, found in 2001 in evaporite rocks in the Chelkar salt dome, W. Kazakhstan. It appears associated with gypsum, anhydrite, halite, bishofite, hilgardite, and magnesite [22]. Its structure solved by single-crystal X-ray diffractometry [23] showed that it must be formulated as $Ca(C_2O_4)\cdot CaCl_2\cdot 2H_2O$.

The only known natural alkaline oxalate is natroxalate, $Na_2(C_2O_4)$, found as a hydrothermal phase in the Lovozero massif, Kola Peninsula, Russia, associated with pyrite, sphalerite, albite, galena, and other minerals [24].

A natural ammonium oxalate, $(NH_4)_2(C_2O_4)\cdot H_2O$, has been found in some guano deposits, often associated with some sulfate minerals of the arcanite–mascagnite series [25].

Different transition metal oxalates have also been found and described. $Fe(C_2O_4)\cdot 2H_2O$, known as humboldtine, is a secondary mineral that occurs in lignite and granite pegmatites

[26] and the isotypic, also secondary mineral, $Mn(C_2O_4)\cdot 2H_2O$ (lindbergite), appears associated with some phosphate minerals [27]. A related trihydrate, $Mn(C_2O_4)\cdot 3H_2O$, was found on small quartz crystals associated with braunite and other manganese minerals, in one location in Switzerland [6, 27]. Besides, moolooite, a hydrated copper oxalate of composition $Cu(C_2O_4)\cdot nH_2O$, probably generated by interaction of oxalic acid from guano and copper sulfides, was found in a Western Australian deposit associated with gypsum, silica, atacamite, whewellite, and other minerals [28]. Another, even rarer mineral is wheatleyite, an hydrated sodium copper oxalate of composition $Na_2[Cu(C_2O_4)_2]\cdot 2H_2O$, probably generated by oxalic acid of animal origin and mine ground waters and found associated to galena, sphalerite, quartz, and a powdered lead oxalate [29].

Some more complex natural oxalates are stepanovite, $NaMg[Fe^{III}(C_2O_4)_3]\cdot 8–9H_2O$, found associated with lignite [3]; the related zemchuzhnikovite, $NaMg[(Al,Fe^{III})(C_2O_4)_3]\cdot 8H_2O$, occurring in chalky clays, and which may be considered as an aluminum stepanovite [30] as well as minguzzite, $K_3[Fe^{III}(C_2O_3)_3]\cdot 3H_2O$, which appears associated to limonite and humboldtine [31, 32].

Another group of interesting oxalate minerals was described some years ago and they are unique in two respects: they are the first natural lanthanide oxalates and the first natural double salts of two acids, one organic and the other inorganic. They appear in cavities as embedded or free-standing crystals mixed with epsomite and the so-called “hair salts”. These minerals are coskrenite, $(Ce,Nd,La)_2(SO_4)_2(C_2O_4)\cdot 8H_2O$ [33], levinsonite, $(Y,Nd,Ce)Al(SO_4)_2(C_2O_4)\cdot 12H_2O$ [34] and zugshunstite, $(Ce,Nd,La)Al(SO_4)_2(C_2O_4)\cdot 12H_2O$ [34]. The last two have a special crystal chemical significance in having the same complex formula type, but different crystal structures, generated by the presence of the lower or higher weight lanthanide cations.

Most recently, a new mineral species named kyanoxalite, with the idealized formula $Na_7[(Al_{5–6}Si_{6–7}O_{24})(C_2O_4)_{0.5–1}]\cdot 5H_2O$, was found in hydrotermally altered hyperalkaline rocks and pegmatites, in the Kola Peninsula, Russia [35]. This mineral represents the first natural alumino-silicate containing an organic acid anion.

2.2. *Metallic oxalates found in plants, fungi and lichens*

Although mineral deposits in plants have been known since the seventeenth century [36], only in the last 50 years their wide distribution in the vegetal kingdom has been unambiguously confirmed. Nevertheless, a complete understanding of the development, distribution, and especially the physiological significance of these mineral deposits has not yet been achieved [6–9].

Calcium oxalate, together with calcium carbonate and opal (hydrated silicon dioxide), are the three most important and largely distributed biominerals in plants [6, 9] and, in particular, calcium oxalates are distributed among all taxonomic levels of photosynthetic organisms from unicellular algae to angiosperms and giant gymnosperms [6, 8] and they are also relatively abundant in fungi [37].

Calcium oxalate biosynthesis is considered to be a basic and important physiological process in higher and lower vascular plants as well as in algae and fungi and accounts for most of the calcium present in some species. It occurs in crystalline form as intracellular or extracellular deposits, adopting different sizes and morphologies. Specialized cells, known as crystal idioblasts, are necessary for calcium oxalate generation, showing features that are adequate for Ca(II) accumulation and for the control and regulation of crystal nucleation

and growth. Therefore, calcium oxalate biomineralization constitutes a good example of a biologically controlled process [2, 4, 5, 9] and both, the chemical nature and crystal phenotype, as well as their localization within the plant body, are under strict genetic control [9].

Both, whewellite, $Ca(C_2O_4)\cdot H_2O$, and weddellite, $Ca(C_2O_4)\cdot 2H_2O$, have been found in plants and fungi [9], although in this last case the formation of the dihydrate seems to be more common [9, 37]. The trihydrate has never been found in plants or in other biological systems, but it may be a precursor of the two lower hydrates [9].

Calcium oxalates have also been found in lichens, although lichens have usually been investigated in relation to rock weathering processes in which this and other metallic oxalates are generated at the lichen–rock interface [6, 9, 38–41]. In these cases, the interaction of oxalic acid generated by the lichens with rock components may be the principal route that originates these biomineral deposits. This means that in these cases, the biomineralization mechanism is of the biological-induced type [2, 4, 5, 9]. Obviously, a close relationship exists between the chemical nature of the substrate and the type of insoluble oxalate that is accumulated immediately beneath or within the thallus. On calcareous rocks, such as limestone or dolomite, as well as on rocks containing calcium-bearing minerals, calcium oxalate is predominant and whewellite and/or weddellite are usually produced [9, 39, 40]. In rocks in which calcium is present in low amounts, other oxalates may be generated.

Accumulation of $Mn(C_2O_4)\cdot 2H_2O$ could be observed during the interaction of the lichen *Pertusaria corallina* with manganese-rich ores [9, 41]. On the other hand, vivid blue inclusions in whewellite or weddellite, occurring in different lichens growing on cupriferous substrates, were identified as moolooite, $Cu(C_2O_4)\cdot nH_2O$ [9, 42]. The generation of $Zn(C_2O_4)\cdot 2H_2O$, as a consequence of lichen or fungal activity has also been observed, whereas the formation of biogenic $Pb(C_2O_4)\cdot 2H_2O$ was demonstrated by *in vitro* experiments [9]. Interestingly, the generation of $Fe(C_2O_4)\cdot 2H_2O$ could never be demonstrated at mineral/lichen interfaces and, therefore, one may speculate that possibly a microbial oxidation of Fe(II) to Fe(III) occurs, followed by hydrolysis and precipitation of iron(III) oxides or oxo-hydroxides [9, 40]. In the case of Fe(III), the formation of soluble oxalates is also possible [9, 39, 43].

Apart from the calcium oxalates discussed above, the dihydrated Mg(II) oxalate, $Mg(C_2O_4)\cdot 2H_2O$, known as glushinskite, surely plays a relatively important role in Nature [9]. This species was also found as a biomineral in the lichen thallus and at the lichen/rock interface of serpentinite (a magnesium silicate with very low calcium content) colonized by *Lecanora atria* [44]. It was also found that Mg(II) can be substituted by small amounts of Fe(II), Mn(II), and Ni(II) [44]. This observation is in agreement with the more general suggestion that a range of previously unreported oxalate biominerals may still exist where oxalic acid-secreting lichens have colonized substrates of appropriate composition [40]. Taking into account that $Mg(C_2O_4)\cdot 2H_2O$ and the dihydrated oxalate complexes of the first-row transition metals are isostructural (cf. section 4.1.3), it seems relatively easy to incorporate the three mentioned cations, and eventually also Zn(II) and Co(II), in the glushinskite lattice [40].

The presence of glushinskite was also revealed in the cactaceae species *Opuntia ellisiana*, associated with whewellie and opal, constituting the first evidence of the presence of this oxalate in plants [45].

Finally, it is interesting to mention that free oxalic acid and some of the soluble oxalates, mainly sodium or potassium oxalates, can also be accumulated in different vegetal tissues. It is well known that certain plant-pathogenic fungi secrete high concentrations of these soluble oxalates as part of the invasive processes [9].

2.3. *Metallic oxalates found in the animal kingdom*

Oxalate biomineralization in animals is mostly associated with a pathological condition: the formation of kidney stones or urolithiasis. Crystalline calcium oxalates, in the form of whewellite or weddellite, are the primary components of urinary stones in both humans and livestock. In animals, oxalate acts as an antinutrient by sequestering Ca(II) and precipitating it in an insoluble form. As animals synthesize only small amounts of oxalate, plant derived oxalates represent the major oxalate source leading to hyperoxaluria, which is a key risk factor for urolithiasis [9].

The biominerals found in kidney stones usually display crystal polymorphism. They consist of pure $Ca(C_2O_4)\cdot H_2O$ or $Ca(C_2O_4)\cdot 2H_2O$, or mixtures of calcium oxalates, calcium phosphates, uric acid and ammonium urate. However, the monohydrate is more frequently present in stones than the dihydrate and results from clinical studies indicate that the formation of $Ca(C_2O_4)\cdot H_2O$ crystals correlate with a more adverse pathology. On the other hand, urolithiasis might be considered an abnormal manifestation of a process that in many other organisms is a normal physiological event that evolved for the control of an excess of oxalate, calcium, or both. Moreover, the formation of calcium oxalate crystals in animals has long been considered as an example of extracellular and non-biologically controlled biomineralization in contrast to plant biomineralization, as discussed above [9].

3. Environmental effects of oxalates

Although oxalate minerals are relatively rare in Nature, the recognition that organic acids are important constituents of some basinal fluids have impact on diagenetic processes and participate in elemental mobilization through complexation, generated increasing research on the environmental effects of these acids and their anions [9, 46]. Acetate with a concentration of up to 10,000 ppm is the most abundant of the dissolved organic acids, constituting between 80 and 90% of total dissolved organic acid species. The remaining anions are basically propionate, butyrate, and valerate, whereas the concentration of oxalate is relatively low [15].

Significant amounts of low-molecular weight dicarboxylic acids (C_2–C_{10}), with predominance of oxalic acid, have been detected during thermal degradation of kerogen and humic acids isolated from lithified sediments. Evidently, these acids play important geochemical roles such as dissolution of carbonates and clay minerals, increasing the permeability and porosity of rocks, and transporting trace metals in the form of complexes [9, 46].

Another interesting aspect is the role of oxalate biominerals in the carbon cycle, although the long-term fate of oxalates and calcium oxalates in natural systems remains uncertain. On the one hand, degradation of oxalates by micro-organisms is a well-established phenomenon that occurs in soils and in the litter below oxalate bearing plants. On the other hand, there is increasing evidence suggesting that calcium oxalate formation is a major pathway leading to calcium carbonate biomineralization [9].

Because oxalic acid is produced as a final product of metabolism by a variety of plants, fungi and animals, it is not surprising that micro-organisms which attack oxalate are widely distributed in Nature [9, 47].

The two major classes of oxalate degrading enzymes found in plants and fungi are oxalate oxidase and oxalate decarboxylase and more than 50 types of oxalotrophic bacteria

have been identified to date [9, 47, 48]. In the context of this review, the first two mentioned enzymes are especially interesting from the point of view of coordination chemistry. They share some common characteristics, as both belong to the cupin superfamily of proteins, are Mn(II) dependent systems, and their active sites show strong similarities [47, 48].

4. Synthetic analogous to the natural metallic oxalates

An important number of the natural oxalates summarized in table 1 has been obtained in the laboratory using different synthetic procedures, and thoroughly investigated by a wide number of physicochemical methods. During these studies, it was also found that in certain cases polymorphic forms and/or closely related hydrates are generated.

Besides, it must be clearly emphasized that not all of these natural oxalates are true coordination compounds as some of them; especially natroxalate, oxamite, and the calcium oxalates are, essentially, ionic compounds.

The oldest and, in certain aspects, classical literature on metallic oxalate complexes was critically analyzed in a very exhaustive review published more than 50 years ago [49].

4.1. *Synthesis and structural characteristics*

4.1.1. Alkali and alkaline-earth oxalates. As mentioned above, natroxalate, $Na_2(C_2O_4)$, is the only crystalline alkali-metal oxalate that occurs naturally. As other simple oxalates, it can be easily obtained by crystallization of the reaction product of Na_2CO_3 with oxalic acid solutions. Commercially it is prepared from the cellulose of sawdust by fusion with NaOH and decomposition of the resulting formate to yield the oxalate, or by reaction of CO_2 with sodium amalgam [49].

The structure of $Na_2(C_2O_4)$ was initially reported by Jeffrey and Parry [50] and later refined by Reed and Olmstead [51]. It belongs to the monoclinic crystal system, space group $P2_1/c$ with $Z = 2$ and the following unit cell dimensions: $a = 3.449(2)°$, $b = 5.243(3)°$, $c = 10.375(4)°$, and $\beta = 92.66(4)°$ [51]. The oxalate anion is planar and the salt has a simple type of ionic lattice structure with a distorted octahedral coordination of oxygen atoms around the sodium cation [50, 51].

Oxalates of the three heavier alkali metal cations can be prepared as the monohydrates by reaction of oxalic acid and the respective carbonates whereas the corresponding anhydrous salts are obtained by dehydration. In $K_2(C_2O_4)$ (orthorhombic, *Pbma*, $Z = 2$), the oxalate anion is planar, whereas in $Cs_2(C_2O_4)$ (monoclinic, $P2_1/c$, $Z = 4$) it is staggered. For rubidium oxalate, two polymorphic forms were found. One of them, β-$Rb_2(C_2O_4)$ (orthorhombic, *Pbma*, $Z = 2$) is isotypic to $K_2(C_2O_4)$, and the other (α-$Rb_2(C_2O_4)$, monoclinic, $P2_1/c$ $Z = 4$) is isotypic to $Cs_2(C_2O_4)$ [52]. The coordination numbers of the cations are clearly dependent on the cationic sizes. Whereas in $Na_2(C_2O_4)$, the coordination polyhedron is, as mentioned, a distorted NaO_6 octahedron; in $K_2(C_2O_4)$ and β-$Rb_2(C_2O_4)$, it is a distorted MO_8 cube and in $Cs_2(C_2O_4)$ and α-$Rb_2(C_2O_4)$, one of the cations presents ninefold coordination whereas the other one is in tenfold coordination [52]. The structure of $Na_2(C_2O_4)$ is, with the exception of the noted differences in coordination numbers, similar to those of $K_2(C_2O_4)$ and β-$Rb_2(C_2O_4)$ [52].

As mentioned in section 2.1, three different hydrates of calcium oxalate can be found in Nature, namely $Ca(C_2O_4)\cdot H_2O$ (whewellite), $Ca(C_2O_4)\cdot 2H_2O$ (weddellite), and $Ca(C_2O_4)\cdot 3H_2O$ (caoxite). As the thermodynamically most stable form, whewellite is the most easily synthesizable hydrate and its formation is enhanced at high temperatures. On the other hand, a number of synthetic strategies has been proposed for the synthesis of all three oxalates, showing the extreme sensitivity of the composition and morphology of the generated solid phases to the experimental conditions (Ca/oxalate ratio, temperature, ionic strength, presence of inhibitors, way of mixing the reactants, etc.) [53–56]. The monohydrate is usually obtained by the reaction of very diluted $CaCl_2$ and $Na_2(C_2O_4)$ solutions at temperatures of about 70 °C, whereas the trihydrate can only be obtained at relatively low temperatures. The most problematic process corresponds to the formation of pure crystals of the dihydrate, for which generation the presence of certain crystallization inhibitors plays a crucial role. Moreover, well-formed crystals of this hydrate can also be obtained by slow evaporation, at room temperature, of a saturated $Ca(C_2O_4)\cdot H_2O$ solution [54].

From the structural point of view, these three calcium oxalates show some strong similarities, as in all of them the Ca(II) ions are coordinated by eight oxygen atoms, belonging either to oxalate anions or to H_2O molecules, located at the corners of a distorted square antiprism [19]. Crystallographic data are presented in table 2.

The monohydrate is dimorphic, presenting a basic structure, which is stable above 38 °C (monoclinic, space group *C2/m* and $Z = 4$) and a low temperature (derivative) form, which is a superstructure generated by doubling of the *b* unit cell constant of the basic form (monoclinic, space group $P2_1/c$ and $Z = 8$) [19, 57–59].

In weddellite, $Ca(C_2O_4)\cdot(2+x)H_2O$, the fractional waters of hydration (i.e. *x* in the formula) occur zeolitically and do not contribute to the Ca(II) coordination polyhedra [19, 59].

A comparison of the structures of the three hydrates shows that progression from monohydrate to dihydrate to trihydrate is a one-to-one expression of the number of O-atoms contributed by H_2O to the eight-oxygen polyhedron around Ca(II). The transformation of each hydrate to the next lower one implies simply the successive replacement of a water molecule by an oxalate anion (contributing one O-atom) [19, 59, 60]. The water molecules play, obviously, an important role in the formation of hydrogen bonds which have a strong impact on the overall structural characteristics of these hydrates. Regarding the geometry of the oxalate ions present in these structures, they are strictly planar in the basic structure of whewellite and in weddellite, whereas in the derivative whewellite structure and in the trihydrate they are non-planar [19, 59, 60].

Recently, pure anhydrous calcium oxalate could be obtained by careful heating of a $Ca(C_2O_4)\cdot H_2O$ sample up to 370 °C, and additional isothermal storage of the solid at this temperature during 5 h. The structure of this compound was determined by combination of

Table 2. Crystallographic data for calcium oxalates.

Oxalate	S.G.	*Z*	*a*(Å)	*b*(Å)	*c*(Å)	*α*(°)	*β*(°)	*γ*(°)	Ref.
$Ca(C_2O_4)\cdot H_2O$[a]	$P2_1/c$	8	6.290	14.583	10.116	90.0	109.46	90.0	[59]
$Ca(C_2O_4)\cdot H_2O$[b]	*C2/m*	4	6.292	7.295	9.978	90.0	107.04	90.0	[58]
$Ca(C_2O_4)\cdot 2H_2O$	*I4/m*	8	12.371	12.371	7.357	90.0	90.0	90.0	[59]
$Ca(C_2O_4)\cdot 3H_2O$	*P(-1)*	2	7.145	8.600	6.099	112.30	108.87	89.92	[60]
$Ca(C_2O_4)$	*P2/m*	4	6.1644	7.3623	9.5371	90.0	90.34	90.0	[61]

[a]Derivative structure.
[b]Basic structure.

atomistic computer simulations and Rietveld refinement of its X-ray powder diagram [61]. Crystallographic data of this oxalate are also included in table 2. The structure is closely related to that of whewellite [61].

The rarest of all the naturally occurring calcium oxalates is novgorodovaite [22], which according to a crystallographic structural analysis can be formulated as $Ca(C_2O_4)\cdot CaCl_2\cdot 2H_2O$ [23]. It belongs to the monoclinic crystal system, space group *I2/m*, with $Z = 2$ and unit cell parameters: $a = 6.936(3)$, $b = 7.382(3)$, $c = 7.443(3)$ Å, and $\beta = 94.3(1)°$. Also in this case the coordination sphere around the Ca(II) ion is a distorted tetragonal antiprism conformed by Cl-atoms and O-atoms from the water molecules and the oxalate anions. An analogous synthetic compound can be obtained by digesting $Ca(C_2O_4)\cdot H_2O$ with a concentrated HCl solution at 100 °C in a securely stoppered flask [62]. A slight modification of this synthetic procedure allows the preparation of another hydrate, namely $Ca(C_2O_4)\cdot CaCl_2\cdot 7H_2O$ [62].

Oxalates for the other alkaline-earth cations have also been prepared and characterized. For Ba(II), a number of hydrated oxalates are known, i.e. $Ba(C_2O_4)\cdot 3.5H_2O$, $Ba(C_2O_4)\cdot 2H_2O$, $Ba(C_2O_4)\cdot H_2O$, $Ba(C_2O_4)\cdot 0.5H_2O$ [63] as well as two modifications of the anhydrous compound [63–65]. In the case of strontium, two different hydrates and the anhydrous oxalate have been reported and, interestingly, the tetragonal $Sr(C_2O_4)\cdot 2H_2O$ is isostructural with weddellite, also containing a small portion of zeolitic water [66, 67]. The monohydrate, $Sr(C_2O_4)\cdot H_2O$, belongs to the triclinic crystal system (space group *P(-1)* and $Z = 2$) [67], whereas $Sr(C_2O_4)$ is monoclinic (space group *C2/c* and $Z = 4$) [68]. The preparation of beryllium oxalate is relatively complex; staring with $BeSO_4\cdot 4H_2O$, it involves the preliminary generation of $Be(OH)_2$ and $Be(OH)_2\cdot 2BeCO_3$ and finally this basic carbonate is dissolved in a slight excess of oxalic acid. The salt is obtained by slow evaporation of this solution in the form of $Be(C_2O_4)\cdot 3H_2O$, although it can also exist as a monohydrate or as a combination of both hydrates, depending on the partial pressure of water vapor above the sample [69]. A basic beryllium oxalate of composition $K_3[Be_3(OH)_3(C_2O_4)_3]\cdot 3H_2O$ has also been prepared and characterized [70]. The structures of all these complexes remain unknown.

4.1.2. Ammonium oxalate. The synthesis of this oxalate is very easy, as it can be obtained by reaction of solutions of oxalic acid with ammonium carbonate or bicarbonate. The structure of the generated $(NH_4)_2(C_2O_4)\cdot H_2O$ has been reported by different authors in the past [6, 71, 72] and later refined by low-temperature (30 K) diffraction measurements [73], complemented by 3-D neutron and X-ray structural studies of both, the protonated and deuterated forms [74].

This oxalate salt belongs to the orthorhombic $P2_12_12$ space group with $Z = 2$ (unit cell parameters $a = 8.035(4)$, $b = 10.309(4)$, $c = 3.795(2)$ Å) and the oxalate anion is twisted by about 26°, with no substantial change in the value of this angle with temperature variation [73] a behavior which is most likely a consequence of the strong hydrogen bonding present in this structure. As the space group $P2_12_12$ contains neither mirror planes nor a center of symmetry, it is predicted that $(NH_4)_2(C_2O_4)\cdot H_2O$ crystals are optically active and will rotate the plane of polarized light passing along its optical axis [75].

4.1.3. First-row dihydrated divalent transition metal oxalates. The dihydrated metallic oxalates of stoichiometry $M^{II}(C_2O_4)\cdot 2H_2O$, with M^{II}=Mg, Fe, Co, and Ni present two polymorphic forms, called α-modification (monoclinic, space group *C2/c* and $Z = 4$) and

β-modification (orthorhombic, space group *Cccm* and $Z = 8$) [76–78], generated from the bidimensional structural arrangement depicted in figure 1, with the oxalate anions acting as tetradentate (bridging) ligands. The structure is complemented with two water molecules, above and below each cation, generating an approximately octahedral $M^{II}O_6$ coordination sphere around the metallic centers [3, 6, 76–78]. These chains generate ordered sheets lying perpendicularly to the *c*-axis of the unit cell [78]. The two polymorphic forms originate in small differences of the 3-D piling up of successive sheets, which causes a reordering of the hydrogen bonds between sheets [78]. Thermodynamically, the α-modification is the most stable form and the $\beta \rightarrow \alpha$ transformation is irreversible [76].

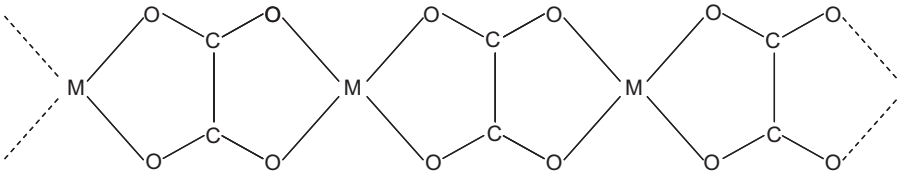

Figure 1. Schematic drawing of the infinite chain arrangement present in divalent metal cation oxalates of the type $M^{II}(C_2O_4)\cdot 2H_2O$.

In the case of $M^{II} = Mn$, two other complex species (γ-$Mn(C_2O_4)\cdot 2H_2O$ and $Mn(C_2O_4)\cdot 3H_2O$), together with the characteristic α-modification are known [79] and, in the case of $M^{II} = Zn$ only the *α*-form has been characterized [77, 78]. Some other hydrates have also been obtained in the case of the Mn(II), Co(II), and Ni(II) oxalates (cf. section 4.1.4).

For the preparation of the two polymorphic forms of these complexes the following general synthetic procedures can be adopted [76, 77]: for the *α*-form, one reacts a soluble salt of the cation with a slight excess of oxalic acid or an alkaline oxalate; for Mg(II), Mn(II), Zn(II), and Fe(II), the reaction can be performed directly at room temperature, whereas for Co(II) the preparation is usually performed at 50–60 °C and for Ni(II), extended heating under reflux is necessary. The β-modifications are obtained by the same reaction, but working with a defect of oxalate and boiling the mixture during reaction.

The structures of these complexes were originally proposed on the basis of the analysis of X-ray powder diffractograms [76–78, 80, 81]. Most recently, the α-modifications of the Mn(II) [82], Fe(II) [83], and Co(II) [84] complexes were investigated by single-crystal X-ray diffractometry. In the case of the complexes belonging to the β-modification, only for β-$Mg(C_2O_4)\cdot 2H_2O$ single-crystal data have so far been reported [85]. Besides, this study

Table 3. Crystallographic data for the two modifications of the $M^{II}C_2O_4\cdot 2H_2O$ complexes.

Oxalate	S.G.	*Z*	*a*(Å)	*b*(Å)	*c*(Å)	*β*(°)	Ref.
α-$Mn(C_2O_4)\cdot 2H_2O$	*C2/c*	4	11.7648	5.6550	9.6367	125.843	[82]
α-$Fe(C_2O_4)\cdot 2H_2O$	*C2/c*	4	12.011	5.557	9.920	128.53	[83]
β-$Fe(C_2O_4)\cdot 2H_2O$	*Cccm*	8	12.26	5.57	15.48	–	[76]
α-$Co(C_2O_4)\cdot 2H_2O$	*C2/c*	4	11.707	5.4487	9.6477	126.155	[84]
β-$Co(C_2O_4)\cdot 2H_2O$	*Cccm*	8	11.877	5.419	15.623	–	[77]
α-$Ni(C_2O_4)\cdot 2H_2O$	*C2/c*	4	11.71	5.33	9.86	127.58	[78]
β-$Ni(C_2O_4)\cdot 2H_2O$	*Cccm*	8	11.842	5.344	15.715	–	[77]
α-$Zn(C_2O_4)\cdot 2H_2O$	*C2/c*	4	11.82	5.41	9.92	127.75	[78]
α-$Mg(C_2O_4)\cdot 2H_2O$	*C2/c*	4	12.68	5.39	9.97	129.5	[78]
β-$Mg(C_2O_4)\cdot 2H_2O$	*Fddd*	8	5.3940	12.691	15.399	–	[85]

allowed for the first time to support the close structural relationship between both crystalline modifications as the *C2/c* space group, characteristic of the α-forms, is a translational subgroup of the *Fddd* space group determined for β-$Mg(C_2O_4)\cdot 2H_2O$ [85].

Crystallographic data for all these complexes are shown in table 3.

4.1.4. Other related first-row divalent transition metal oxalates. In the case of Cu(II), an oxalate of composition $Cu(C_2O_4)\cdot nH_2O$ (synthetic mooloite) can be obtained by slow addition of a solution of oxalic acid to a boiling solution of $CuSO_4\cdot 5H_2O$, with continuous stirring [86]. The water content of these samples is usually small ($n = 0.5$–1) [86, 87] and it is, apparently, of "zeolitic" nature [28, 87]. As so far all attempts to grow single crystals adequate for structural studies have been unsuccessful, the only available structural information is derived from an EXAFS study [88]. This study points to a ribbon structure similar to that depicted in figure 1, with a square planar coordination of the Cu(II) cation. For the first shell, the four Cu–O distances are within 1.98(2) Å and the Cu–Cu distances are of the order of 5.14 Å [88].

As mentioned above, in the case of Mn(II), apart from the α-$Mn(C_2O_4)\cdot 2H_2O$, two other hydrates could be characterized, namely γ-$Mn(C_2O_4)\cdot 2H_2O$ and $Mn(C_2O_4)\cdot 3H_2O$ [79]. The trihydrate is obtained at room temperature by slow addition of a diluted manganese(II) acetate solution over another containing the stoichiometric amount of oxalic acid. After completeness of the addition, a pink precipitate of the complex is formed. Boiling the suspension, containing the trihydrate for a short time, generates the α-$Mn(C_2O_4)\cdot 2H_2O$. Working at a somewhat higher pH-value, which can be simply obtained using diluted ammonium oxalate and manganese(II) nitrate solutions, and heating the reaction mixture at 80 °C overnight generates the γ-$Mn(C_2O_4)\cdot 2H_2O$ [79].

This γ-$Mn(C_2O_4)\cdot 2H_2O$ modification crystallizes in the orthorhombic space group $P2_12_12_1$ with $a = 6.262(4)$, $b = 13.585(5)$, and $c = 6.091(4)$ Å, and $Z = 4$. It presents also a chain structure, but different to that depicted in figure 1. The Mn(II) cations are also in distorted octahedral environments, bonded to two water molecules in *trans* positions and to four oxalate oxygens. One of these oxalate oxygens remains non-bonded whereas another binds to two cations and, therefore, the octahedra share corners, forming chains along the *c* axis of the unit cell [89].

The structure of the trihydrate, better formulated as $[MnC_2O_4(H_2O)_2]\cdot H_2O$, was reported some years ago independently by two different research groups [90, 91]. It belongs to the orthorhombic crystal system, space group *Pcca*, with $a = 9.7660(9)$, $b = 6.6155(6)$, and $c = 10.5192(10)$ Å, and $Z = 4$ [91]. In this case, the structure can be described as a 1-D *zig-zag* chain in which the Mn(II) cations are bis-bidentately bridged by oxalate groups. Water molecules in this hydrate are of two kinds. Two-thirds of them are coordinated with Mn(II) ions, and the rest is present as lattice water. However, the most exciting fact of this structure is that the two coordinated water molecules, as shown in figure 2, are in *cis* positions to another, instead of the typical *trans* arrangement found in the α-$M^{II}(C_2O_4)\cdot 2H_2O$ and β-$M^{II}(C_2O_4)\cdot 2H_2O$ forms of the dihydrated complexes.

The trihydrate is relatively unstable, especially when it is not completely dry. In this case, conversion to α-$MnC_2O_4\cdot 2H_2O$ occurs within a few days [79]. When the hydrated manganese oxalates are heated *in vacuo* at moderate temperatures, they transform into the anhydrous oxalate, which is so far not well characterized from the structural point of view [79].

Another closely related manganese(II) oxalate is the complex $[Mn_2(C_2O_4)(OH)_2]$, obtained by hydrothermal reaction, at 160 °C, of mixtures of $MnC_2O_4\cdot 2H_2O$, piperazine

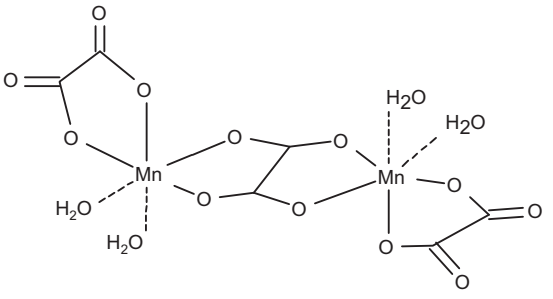

Figure 2. Schematic drawing of the Mn(II) environment in $[MnC_2O_4(H_2O)_2]\cdot H_2O$.

and water [89]. It presents a very complex tridimensional structure, consisting of manganese–oxygen layers, linked by bridging and chelating oxalates but in this case each oxalate ligand coordinates to four Mn(II) centers. Each Mn(II) cation is bonded to three (meridional) hydroxides, a chelating oxalate and a monodentate oxalate, generating a highly distorted octahedral environment. Besides, the OH-ions bridges between three Mn(II) ions [89].

More than 30 years ago it was shown that, under certain experimental conditions, it is possible to obtain the Co(II) oxalate as a tetrahydrate, which slowly transforms into the dihydrate [92]. Most recently, this tetrahydrate, which must be better formulated as $[Co(C_2O_4)(H_2O)_2]\cdot 2H_2O$, could be obtained in crystalline form and was structurally characterized. For its preparation, a methanolic solution of 4-amine-1,2,4-triazole is slowly diffused into an aqueous solution containing $Co(C_2O_4)\cdot 2H_2O$ and $K_2(C_2O_4)\cdot H_2O$. After two weeks red crystals of the tetrahydrate are generated [93].

$[Co(C_2O_4)(H_2O)_2]\cdot 2H_2O$ crystallizes in the triclinic space group $P\,\bar{1}$ with cell parameters $a = 6.627(2)$, $b = 8.715(2)$, $c = 11.106(2)$ Å, $\alpha = 69.86(1)°$, $\beta = 83.45(1)°$, $\gamma = 72.33(1)°$, and $Z = 3$. The structure has the same 1-D linear chain arrangement as that of the two dihydrated Co(II) complexes described in section 4.1.3, and contains, additionally, two H_2O molecules as crystallization waters [93].

Interestingly, in the case of Ni(II) oxalate, it is possible to obtain a third dihydrated form by solvothermal synthesis, using the amino acid L-serine as the carboxylate source [94]. The obtained $Ni(C_2O_4)\cdot 2H_2O$ crystallizes, curiously, in the same space group as α-Ni $(C_2O_4)\cdot 2H_2O$ (*C2/c*) with unit cell parameters $a = 13.419$, $b = 6.562$, $c = 10.359$, $\beta = 138.94$, and $Z = 4$. The chain backbone, constructed by bis-chelating oxalate ligands, presents a *zig-zag* chain in the [101] direction. The Ni(II) cations have a distorted octahedral geometry, surrounded by six oxygen atoms, four of them from two different oxalate moieties and the other two from *cis* coordinated water molecules [94].

In the case of Fe(II), also a complex oxalate of stoichiometry $[Fe_2(C_2O_4)(OH)_2]$, isostructural with the similar Mn(II) complex described above, could be obtained by hydrothermal synthesis [95]. It can be admitted that this complex bears a direct relation to humboldtine and may be generated by decomposition of this complex according to [95]:

$$2Fe(C_2O_4)\cdot 2H_2O \longrightarrow [Fe_2(C_2O_4)(OH)_2] + C_2O_4H_2 + 2H_2O$$

Although not found in Nature, another directly related divalent metal oxalate, which merits a brief comment, is $Cd(C_2O_4)\cdot 3H_2O$. This oxalate can be precipitated in the form of a

microcrystalline powder by mixing diluted aqueous solutions of cadmium(II) acetate and oxalic acid, at 65 °C, under continuous stirring [96]. Small single crystals, adequate for X-ray diffractometric studies, can be obtained by controlled diffusion of Cd(II) ions through silica-gel impregnated with oxalic acid [97] or by *in situ* generation of oxalic acid in the presence of aqueous Cd(II) solutions, using either oxalylhydroxamic acid [98] or L-ascorbic acid [99].

The polymeric structure of $CdC_2O_4 \cdot 3H_2O$ is triclinic, space group *P1* and $Z = 2$ and consists of 2-D arrays formed by a $Cd_2(C_2O_4)_2 \cdot 6H_2O$ repeat unit, where both of the symmetry-independent Cd(II) cations are in a seven-coordinate environment of five oxalate and two water oxygens. Two additional H_2O molecules of the repeat unit are uncoordinated but are involved in the hydrogen bond network present in the structure [99]. Interestingly, a structurally related $Pb(C_2O_4) \cdot 3H_2O$ complex has also been reported [98] and in this case also a dihydrate, $Pb(C_2O_4) \cdot 2H_2O$ [100], and the anhydrous $Pb(C_2O_4)$ [101, 102], have been investigated.

In the context of the metal–oxalate chains discussed in this section, it is also valuable to mention that an important number of oxalato complexes of this type with a variety of secondary ligands, completing the coordination sphere of the metal center, has been prepared and characterized during the last years. A few examples of this kind of complexes are briefly discussed as follows.

In the case of $Cu(C_2O_4) \cdot (pyOH)_2$ (pyOH = 3-hydroxyppyridine), each Cu(II) cation is six-coordinated by four oxygen atoms belonging to two bridging oxalato ligands and two nitrogen atoms from the two pyOH molecules. These two ligands are in *cis*-position and the polymeric chain presents a *zig-zag* conformation [103].

Another somewhat more complex structure is found in the case of $[Cu_2(C_2O_4)_2(ampy)_3] \cdot ampy$ (ampy = 2-amino-4-methylpyridine). The structure consists of free ampy molecules and chains of copper(II) ions, bridged by bis(chelating) oxalato ligands and two crystallographically independent Cu(II) ions [Cu(1) and Cu(2)] alternate regularly within this chain, in which two slightly different bidentate oxalate groups are found, in contrast to what occurs in the previously discussed complexes in which all the oxalate ligands are equivalent. Four O-atoms from two bridging oxalate anions and two *cis*-coordinated pyridinic N-atoms from two ampy ligands build an elongated octahedral surrounding around Cu(1). The environment around Cu(2) is a distorted square pyramid with four oxalate–oxygen atoms in the basal plane and the pyridine nitrogen atom from one ampy molecule in the apical position [104].

Another interesting series of related complexes have been obtained by the reaction of $M(C_2O_4) \cdot 2H_2O$ (M = Co(II), Ni(II)) or $K_2[Cu(C_2O_4)_2] \cdot 2H_2O$ with *n*-ampy ($n = 2,3,4$; *n*-ampy = *n*-aminopyridine) and potassium oxalate. In all cases, 1-D oxalato-bridged metal(II) complexes are obtained, with the coordination sphere of the metal centers completed by a pair of aromatic bases [104].

Four groups of complexes are obtained:

- $M(C_2O_4) \cdot 2$(2-ampy): M = Co, Ni, and Cu; space group *C2/c*, and $Z = 4$; and 2-ampy *cis*-coordinated.
- $M(C_2O_4) \cdot 2$(3-ampy): M = Co, No, and Cu; space group *Pcnn*, and $Z = 8$; and 3-ampy *cis*-coordinated.
- $Co(C_2O_4) \cdot 2$(4-ampy): space group *C2/c* and $Z = 4$; and 4-ampy *trans*-coordinated.
- $M(C_2O_4) \cdot 2$(4-ampy): M = Ni, Cu; space group *Fddd* and $Z = 8$; and 4-ampy *trans*-coordinated.

Other two similar related complexes are $Fe(C_2O_4)\cdot DPA$ and $Ni(C_2O_4)\cdot DPA$ (DPA = 2,2-dipyridylamine) obtained by hydrothermal synthesis of a mixture of the respective metal dibromides, oxalic acid and DPA in water. Their structures consist of octahedral metal centers surrounded by two tetradentate oxalates and one bidentate DPA moiety, extended as unidimensional *zig-zag* chains [105]. Some other interesting complexes derived from unidimensional oxalate *zig-zag* chains are $Zn(C_2O_4)\cdot bipy$ [106], $Co(C_2O_4)\cdot bipy$ [107] (bipy = 2,2′-bipyridine), and $Cu(C_2O_4)\cdot ophen$ (ophen = 1,10-phenanthroline) [108], in which the metal centers present also a distorted octahedral coordination, conformed by four oxalate O-atoms, of two different bidentate oxalate moieties and the two N-atoms of the bidentate organic ligands (bipy or ophen).

Finally, it must be mentioned that the thermal decomposition of the dihydrated oxalates of Fe(II), Co(II), Ni(II), Zn(II), and Cu(II) allows the generation of the respective anhydrous compounds. They can be obtained in two forms, a disordered one, denominated α-MC_2O_4, or an ordered one, called β-MC_2O_4 [109]. The ordered forms were investigated in detail. They belong to the monoclinic $P2_1/n$ space group with $Z = 2$ and their structures can also be derived from the chain structure depicted in figure 1. Each M(II) ion is in a highly distorted octahedral coordination conformed by four O-atoms in its own chain and by other two O-atoms from adjacent chains (at a somewhat greater distance). Consequently, in this structure the chains are interlinked generating a tridimensional array [109, 110]. A similar β-CdC_2O_4 oxalate can only be obtained by hydrothermal synthesis, but not by the thermolysis of $CdC_2O_4\cdot 3H_2O$ [111].

4.1.5. Synthetic wheatleyite and related complexes. Synthetic wheatleyite, $Na_2[Cu(C_2O_4)_2]\cdot 2H_2O$, and the analogous potassium and ammonium compounds, could be easily obtained by dissolution of $Cu(C_2O_4)\cdot nH_2O$ in a warm (ca. 50 °C) aqueous solution of the respective monovalent cation oxalate up to a final molar ratio soluble oxalate/Cu $(C_2O_4)\cdot nH_2O$ equal to 2 [112]. Besides, $Rb_2[Cu(C_2O_4)_2]\cdot 2H_2O$ is obtained by a more complex procedure, i.e. by slow evaporation of aqueous solutions containing Rb_2CO_3, $CuCl_2$, basic copper carbonate, $H_2C_2O_4\cdot 2H_2O$, and HNO_3 (final pH-value 8) [113]. In the case of $Cs_2[Cu(C_2O_4)_2]\cdot 2H_2O$, the synthetic procedure was not described [114], but it can probably be obtained by a similar reaction as the rubidium compound.

The $Na_2[Cu(C_2O_4)_2]\cdot 2H_2O$ salt crystallizes in the triclinic space group $P\bar{1}$ with $Z = 1$ [29, 115]; whereas the respective potassium [116], ammonium [117], rubidium [113], and cesium [114] salts, which are isostructural, also belong to the same space group but with $Z = 2$. Crystallographic data for the five complexes are shown in table 4. The structure of $Na_2[Cu(C_2O_4)_2]\cdot 2H_2O$ consists of stacked, quasi-planar $[Cu(C_2O_4)_2]^{2-}$ units and linear chains of Na^+ cations and H_2O molecules running parallel to the *c* axis of the unit cell. As

Table 4. Crystallographic data for the $M^I_2Cu(C_2O_4)_2\cdot 2H_2O$ complexes (M^I = Na, K, NH_4, Rb, and Cs).

M^I	S.G.	Z	a	b	c	α	β	γ	Ref.
Na^+	$P\bar{1}$	1	7.535	9.473	3.576	81.90	103.77	108.09	[115]
K^+	$P\bar{1}$	2	8.7092	10.3904	6.9486	121.110	82.956	110.848	[116]
NH_4^+	$P\bar{1}$	2	8.91	10.65	6.95	122.58	85.87	109.0	[117]
[a]Rb^+	$P\bar{1}$	2	7.000	8.949	8.982	108.05	97.69	97.99	[113]
Cs^+	$P\bar{1}$	2	9.2980	9.1167	7.1316	97.524	97.410	107.522	[114]

[a]A standard (reduced) unit cell was used in this case, whereas the structural models of the K, NH_4, and Cs salts were described using a non-standard unit cell [113].

shown in figure 3(A), the Cu(II) ion lie on a center of symmetry and is coordinated to two oxalate anions, each acting as a bidentate ligand and generating a practically square CuO_4 moiety. The environment of copper is completed with two centrosymmetrically related oxygen atoms from neighboring $[Cu(C_2O_4)_2]^{2-}$ groups, one above and one below, in the same stack [115]. Thus, the Cu(II) cations may be considered as being inserted in an distorted octahedron elongated by the Jahn–Teller effect.

As shown in figure 3(B), the structures of $K_2[Cu(C_2O_4)_2]\cdot 2H_2O$ and of the isotypic NH_4^+, Rb^+, and Cs^+ salts contain two types of building units: $[CuC_2O_4)_2(H_2O)_2]^{2-}$ and $[Cu(C_2O_4)_2]^{2-}$ groups, disposed in such a way that the additional interaction on the Cu(II) ions of the second unit occurs through weak oxalate bridges, involving free O-atoms of the oxalate ligands of the first unit. This means that in both types of complex moieties, the Cu(II) cation lies in a distorted CuO_6 octahedral coordination [115].

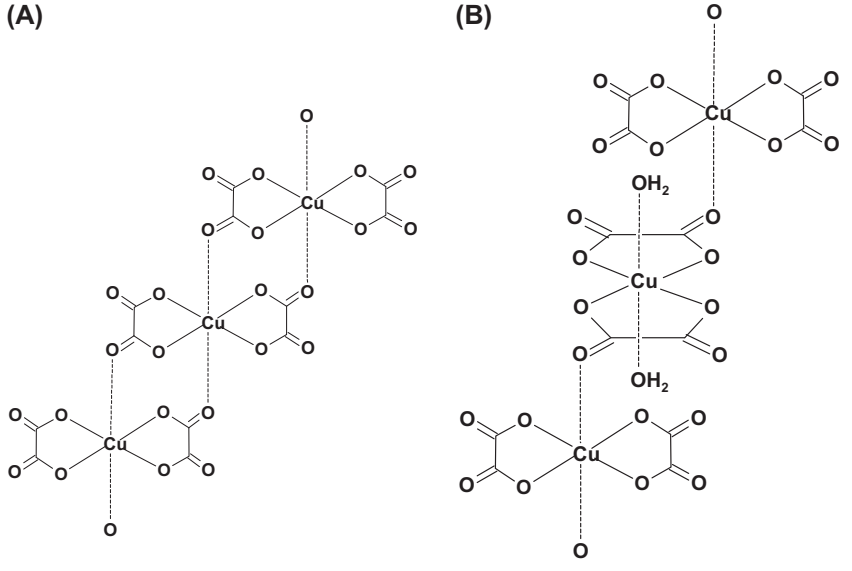

Figure 3. Schematic drawing of the structural units in $Na_2Cu(C_2O_4)_2\cdot 2H_2O$ (A) and in the respective K, Rb, Cs, and NH_4 salts (B).

4.1.6. Oxalato complexes containing Fe(III). The synthetic analogous complex to the mineral minguzzite is one of the best known Fe(III) oxalate complexes, the tri-hydrated potassium *tris*(oxalato) ferrate(III), $K_3[Fe(C_2O_4)_3]\cdot 3H_2O$. This complex can be easily obtained by different synthetic procedures some of which are briefly mentioned here: (a) by H_2O_2 oxidation of Fe(II) oxalate in the presence of oxalic acid and potassium oxalate [118]; (b) by direct interaction of $FeCl_3$ and $K_2(C_2O_4)\cdot H_2O$ solutions [119]; and (c) by digestion over a steam bath of a mixture of ferric sulfate, barium oxalate, and $K_2(C_2O_4)\cdot H_2O$ [120]. This last procedure, developed in *Inorganic Synthesis*, can also be applied, with slight modifications, to the preparation of the similar complexes of Cr(III) and Al(III). The light-green colored $K_3[Fe(C_2O_4)_3]\cdot 3H_2O$ is photosensitive, the oxalate ligand being be oxidized to CO_2 with concomitant reduction of Fe(III)–Fe(II) [121].

The crystal structure of $K_3[Fe(C_2O_4)_3]\cdot 3H_2O$ has been solved many years ago. It belongs to the monoclinic space group $P2_1/c$ with $Z = 4$ and has the following unit cell parameters: $a = 7.66(2)$, $b = 19.87(1)$, $c = 10.27(2)$ Å, and $\beta = 105.05°$ [122]. This complex is isostructural with the respective Al(III), Cr(III), and Ru(III) complexes [122] and the metal centers present an octahedral $M^{III}O_6$-coordination generated by O-atoms of the three oxalato ligands, with the water molecules intercalated between these octahedra and participating in hydrogen bonds that stabilize the structural arrangements.

The crystal structures of $K_3[Cr(C_2O_4)_3]\cdot 3H_2O$ [123, 124] and of $K_3[Al(C_2O_4)_3]\cdot 3H_2O$ [122, 124] have also been determined, confirming the close structural relation to $K_3[Fe(C_2O_4)_3]\cdot 3H_2O$.

On the other hand, the anhydrous $K_3[Fe(C_2O_4)_3]$ could be obtained and characterized very recently, too. It crystallizes in the chiral space group $P4_132$ of cubic symmetry with $a = 13.5970(2)$ Å and $Z = 4$ and the Fe(III) cation lies again in a distorted octahedral FeO_6 environment [125].

Synthetic complexes analogous to the minerals stepanovite, $NaMg[Fe^{III}(C_2O_4)_3]\cdot 8–9H_2O$, and zhemchuzhnikovite, $NaMg[(Al,Fe^{III})(C_2O_4)_3]\cdot 8H_2O$, have never been described as such. Notwithstanding, a complex species of composition $NaMg[Al(C_2O_4)_3]\cdot 8H_2O$ is well known and has often been used as a host material for different spectroscopic studies.

$NaMg[Al(C_2O_4)_3]\cdot nH_2O$ ($n = 8$ or 9) can be obtained from the reaction in water of stoichiometric amounts of $Al_2(SO_4)_3$, $Ba(OH)_2$, NaOH, MgO, and $H_2C_2O_4\cdot 2H_2O$. Large single crystals were readily grown by evaporation. Part of the Al(III) can be easily replaced by other trivalent cations (Ti, V, Cr, Mn, Fe, and Co) [126]. In this way, it becomes possible to generate synthetic zhemchuzhnikovite, replacing part of the Al(III) by Fe(III), whereas the total replacement allows the generation of synthetic stepanovite.

As far as we know, detailed structural studies on any of these complexes have not been performed yet. Only the crystal structure of the related $NaMg[Cr^{III}(C_2O_4)_3]\cdot 8H_2O$ complex has been determined by single-crystal X-ray diffractometry and the space group was found to be $P\bar{3}1c$ with two formula units per primitive hexagonal unit cell ($a = 9.78(4)$ and $c = 12.47(21)$ Å) [127], and it can be admitted that all the other, related complexes, may posses the same structure [128]. Besides, another independent structural study of $NaMg[Cr^{III}(C_2O_4)_3]\cdot 8H_2O$ suggested an eventually greater unit cell, containing six formula units, and with the space group $P\bar{3}c1$ or $P3c1$ [129]. This assumption can eventually be extended to the two mineral species (stepanovite and zhemchuzhnikovite) for which trigonal symmetry and $Z = 6$ were reported [130].

In relation to all the above-mentioned Fe(III) complexes, it is also interesting to make some comments on the simple iron(III) oxalate, $Fe_2(C_2O_4)_3\cdot 4H_2O$. This oxalate can be easily obtained reacting freshly precipitated ferric hydroxide with oxalic acid [131].

Up to now, it was impossible to obtain single crystals of this complex, adequate for X-ray structural studies. Therefore, it was attempted to attain an insight into its structure, using spectroscopic methodologies. The analysis of the FTIR and Raman spectra suggests the presence of terminal carbonyl groups and excludes the possibility of an ionic structure. On the other hand, for stoichiometric reasons the formation of a dimeric complex must be expected. As the corresponding ^{57}Fe-Mössbauer spectrum confirmed the equivalence of these dimeric sites as well as an octahedral coordination for them, one plausible structural arrangement may be one similar to that depicted in figure 1, but containing only one pair of metallic centers, disrupting the polymeric structure. As shown in figure 4, this implies the presence of a central (tetradentate) oxalate ligand bridging the two Fe(III) cations, and two terminal (bidentate) oxalate ligands, each interacting with only one of the metal centers.

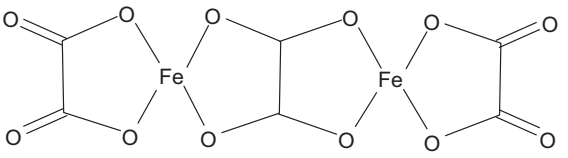

Figure 4. Fe(III)/oxalate linkage in the structure proposed for $Fe_2(C_2O_4)_3 \cdot 4H_2O$.

The coordination of each cation is completed again by two water molecules, lying perpendicularly to the iron/oxalate linkage [132].

4.1.7. Lanthanide sulfato–oxalato complexes. As mentioned in section 2.1, the minerals coskrenite, levinsonite, and zugshunstite are complexes of lanthanide cations simultaneously bonded to organic (oxalato) and inorganic (sulfato) ligands and are the only species of this type so far reported and characterized [133]. The crystal structures of the three minerals have been solved by single-crystal X-ray diffractometry and its main characteristics are discussed as follows:

Coskrenite, $(Ce,Nd,La)_2(SO_4)_2(C_2O_4)\cdot 8(H_2O)$, is triclinic, space group $P\bar{1}$, with $a = 6.007(1)$, $b = 8.368(2)$, $c = 9.189(2)$ Å, $\alpha = 99.90(2)°$, $\beta = 105.55(2)°$, and $\gamma = 107.71(2)°$, and $Z = 1$ [33]. The coordination polyhedra around the Ln(III) cations are monocapped square antiprisms, generating LnO_9 units which are linked by corner sharing with SO_4-tetrahedra, forming chains extended along [110]. These chains are further linked through oxalate anions, into sheets parallel to [001] [33, 133]. Four of the O-atoms around each Ln(III) cation are from H_2O molecules, other two from two different bridging SO_4-groups, two from one oxalato ligand and the remaining one from another oxalato anion [33]. This means that the $C_2O_4^{2-}$ ligands are tetradentate, with two of each O-atoms bonded to one Ln(III) cation and each of the other two, to two different cations, i.e. each oxalate ligand is shared by three different cations.

Levinsonite, $(Y,Nd,Ce)Al(SO_4)_2(C_2O_4)\cdot 12H_2O$, and zugshunstite, $(Ce,Nd,La)Al(SO_4)_2(C_2O_4)\cdot 12H_2O$, are closely related minerals The first one crystallizes in the monoclinic space group *P2/n* ($a = 10.289(1)$, $b = 9.234(1)$, $c = 11.015(1)$ Å, $\beta = 108.50(1)°$, and $Z = 2$ whereas the other one is also monoclinic but with space group *C2/c* and $Z = 4$ ($a = 8.718(1)$, $b = 18.313(2)$, $c = 13.128(2)$ Å, and $\beta = 93.90(1)°$) [34]. The Ln(III) coordination polyhedra of levinsonite is a square antiprism defined by eight O-ligands, whereas in zugshunstite, it is a capped square antiprism defined by nine O-ligands. These coordination polyhedra resemble those of xenotime and monazite, respectively [34].

In levinsonite, two of the O-atoms are from coordinated water, two from two different monodentate SO_4-groups, and the other four from two oxalato ligands, which in this case acts as tetradentate, bridging two adjacent LnO_8-polyhedra. Eight of the coordinating atoms in zugshunstite are similar in origin and the cap is an additional O-atom from another water molecule. In both minerals, the Al(III) ions are present as practically "isolated" $[Al(H_2O)_6]^{3+}$ units that are bonded to the building blocks of the structures only through H-bonds [34].

Synthetic complexes of this type have so far not been reported and, in general, lanthanide complexes with mixed oxalate and sulfate ligands are relatively rare [33, 133–135].

5. Thermal properties

The thermal behavior, under different experimental conditions, of much of the here described natural and synthetic metallic oxalates has often been investigated during the last 50 years. As a result of these investigations, it has been suggested that the thermolysis of the divalent-metal oxalato complexes may be classified according to three principal reactions [6, 136, 137], as follows:

$$M(C_2O_4) \longrightarrow MCO_3 + CO$$

$$M(C_2O_4) \longrightarrow MO + CO + CO_2$$

$$M(C_2O_4) \longrightarrow M + 2CO_2$$

What's more, it has also been emphasized that the decomposition routes may be strongly affected by the environment in which reactions take place [137].

5.1. *Thermal behavior of natural oxalates*

The thermal behavior of most of the simplest natural metal oxalates has been investigated in detail in a series of interesting studies by R.L. Frost and coworkers, using high-resolution thermogravimetry (in a flowing N_2 atmosphere) complemented by evolving gas mass spectrometry, Raman microscopy coupled to a thermal stage, and infrared emission spectroscopy. The main results of these investigations are briefly summarized in this section.

During the thermolysis of whewellite, $Ca(C_2O_4)\cdot H_2O$, three mass loss steps were detected to occur at 162, 479, and 684 °C which on the basis of the physicochemical studies may be unambiguously related to the following processes [138]:

$$Ca(C_2O_4) \cdot H_2O \longrightarrow Ca(C_2O_4) + H_2O \quad (T = 162\,^{\circ}C)$$

$$Ca(C_2O_4) \longrightarrow CaCO_3 + CO \quad (T = 479\,^{\circ}C)$$

$$CaCO_3 \longrightarrow CaO + CO_2 \quad (T = 684\,^{\circ}C)$$

For weddellite, $Ca(C_2O_4)\cdot 2H_2O$, and using the same combination of experimental techniques, also three degradation steps were found at 114, 422, and 592 °C. In the first step, the two water molecules were evolved whereas in the other two, liberation of CO and CO_2, in a similar way as for whewellite occurs [139].

In the case of the mineral moolooite, copper(II) oxalate, it was shown that the investigated natural sample is anhydrous, whereas the complete thermal degradation takes place in two steps. In the first one, occurring at 240 °C, formation of CuO was observed ($Cu(C_2O_4) \rightarrow CuO + CO_2 + CO$), followed at about 800 °C by the generation of Cu_2O ($2CuO \rightarrow Cu_2O + \frac{1}{2}O_2$) [140].

In the case of humboldtine, $Fe(C_2O_4)\cdot 2H_2O$, the high-resolution thermogram shows a great complexity, as three decomposition stages with multiple steps are observed. A first step, with two mass losses is observed at 130 and 141 °C, followed by a broad and poorly

defined step centered at 235 °C. The third stage consists of two mass losses at 312 and 332 °C. In agreement with the TG results, mass spectrometry shows that water is liberated in two steps during the first stage. Carbon dioxide is emitted over a broad temperature range, beginning at about 200 °C and the mass spectrum shows clearly two CO_2 peaks at 322 and 354 °C. The process was additionally followed by Raman and IR measurements and all the collected information allowed proposing the following decomposition scheme [141]:

$$Fe(C_2O_4) \cdot 2H_2O \longrightarrow Fe(C_2O_4) \cdot H_2O + H_2O$$

$$Fe(C_2O_4) \cdot H_2O \longrightarrow Fe(C_2O_4) + H_2O$$

Then, the generated anhydrous ferrous oxalate can decompose following two alternative and simultaneous pathways:

$$Fe(C_2O_4) \longrightarrow FeO + CO + CO_2$$

$$\text{and} \qquad Fe(C_2O_4) \longrightarrow FeCO_3 + CO$$

$$FeCO_3 \longrightarrow FeO + CO_2$$

The thermal degradation of the mineral glushinskite, $Mg(C_2O_4)\cdot 2H_2O$, is relatively simple as it presents only two mass loss steps at 148 and 397 °C. The first corresponds to the liberation of the two water molecules, whereas the second one is related to the degradation of the anhydrous oxalate ($Mg(C_2O_4) \rightarrow MgO + CO + CO_2$). Although there is no evidence for the breakdown of this last step into two successive steps, it is possible that the Mg (C_2O_4) decomposed first to $MgCO_3$ and CO with the final breakdown of the carbonate to MgO and CO_2 in a similar way as found for the calcium oxalates [142].

The case of oxammite, $(NH_4)_2(C_2O_4)\cdot H_2O$ is somewhat more complex although the thermogram is also relatively simple and is conformed by three steps, located at 57, 175, and 188 °C. The thorough analysis of the process allowed proposing the following decomposition scheme:

$$(NH_4)_2(C_2O_4) \cdot H_2O \longrightarrow (NH_4)_2C_2O_4 + H_2O \quad (T = 57\,^{\circ}C)$$

$$(NH_4)_2(C_2O_4) \longrightarrow 2NH_3 + H_2C_2O_4 \quad (T = 175\,^{\circ}C)$$

$$H_2C_2O_4 \longrightarrow H_2CO_3 + CO \ \text{ superimposed with } \ H_2CO_3 \longrightarrow H_2O + CO_2 \quad (T = 188\,^{\circ}C)$$

This means that in the first step liberation of water, at a relatively low temperature, takes place. The second step is related to the liberation of ammonia with simultaneous generation of oxalic acid. The last step involves a more complex process as the liberation of CO and CO_2 occurs practically simultaneously [143].

The thermal behavior of all the other minerals summarized in table 1 has so far not been investigated.

5.2. *Thermal behavior of the synthetic oxalates*

As mentioned at the beginning of this section, an important number of studies on the thermal behavior of metallic oxalates have been performed including standard TG/DTA/DSC measurements under different atmospheres and heating rates as well as works under isothermal conditions with the aid to explore mechanistic aspects and to attain kinetic data [136, 137, 144–146]. As it is impossible to present here all this information, we restrict it mainly to the most important stoichiometric and other chemical aspects using, as far as possible, some of the most recent literature data.

Synthetic sodium oxalate has been repeatedly investigated and its thermal decomposition, which in a N_2 atmosphere occurs at about 575 °C [147], is a good example of the generation of carbonate, as the first decomposition step (Na_2 (C_2O_4) → Na_2CO_3 + CO) [137, 147].

The three hydrates of calcium oxalate have often been investigated, especially the monohydrate (synthetic whewellite) which is one of the best and most widely used reference materials in thermal analysis [3, 136, 148]. First studies with the three synthetic oxalates by French authors gave a first insight into their stabilities and showed that the dehydration of the trihydrate to the monohydrate is irreversible whereas the dehydration of $Ca(C_2O_4)\cdot H_2O$ to the anhydrous oxalate is reversible [149, 150].

As an extension of the thermal studies on natural whewellite and weddellite, mentioned in section 5.1, Echigo *et al.* have also investigated the behavior of synthetic caoxite, $Ca(C_2O_4)\cdot 3H_2O$. They found four thermogravimetric weight loss steps at 85.1, 166.9, 424.7, and 724.9 °C, which can be related to the following processes [151]:

$$Ca(C_2O_4)\cdot 3H_2O \longrightarrow Ca(C_2O_4)\cdot H_2O + 2H_2O \quad (85.1\ ^\circ C)$$

$$Ca(C_2O_4)\cdot H_2O \longrightarrow Ca(C_2O_4) + H_2O \quad (166.9\ ^\circ C)$$

$$Ca(C_2O_4) \longrightarrow CaCO_3 + CO \quad (424.7\ ^\circ C)$$

$$CaCO_3 \longrightarrow CaO + CO_2 \quad (724.9\ ^\circ C)$$

On the basis of this information and that derived from the behavior of the mono and the dihydrate, discussed above, it is possible to summarize the thermal behavior of the calcium oxalates as shown in figure 5. As it can be seen, caoxite transforms directly into the monohydrate without the intermediate formation of the dihydrate. The monohydrate dehydrates and transforms into anhydrous calcium oxalate, which hydrates on cooling and returns to whewellite. However, whewellite dos not hydrate into caoxite. On the other hand, the dihydrate dehydrates into the anhydrous oxalate directly, not through the monohydrate. Interestingly, and as mentioned, the anhydrous form hydrates into the monohydrate on cooling, which shows that the dehydration reaction of the dihydrate is irreversible.

Synthetic glushinskite, $Mg(C_2O_4)\cdot 2H_2O$, behaves in the same way as the natural material. As shown by the TG trace after dehydration, which occurs in the temperature range between 110 and 170 °C, at higher temperatures, in the range between 270 and 380 °C, the decomposition of the anhydrous oxalate with formation of MgO takes place [152]. Interestingly, the thermal decomposition of a magnesium oxalate/oleylamine complex, prepared from $Mg(C_2O_4)\cdot 2H_2O$ as a precursor, allows the synthesis of MgO nanocrystals with an average diameter of about 20–25 nm [152].

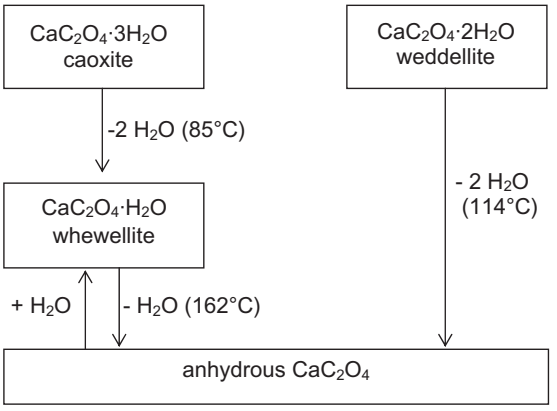

Figure 5. Thermal behavior of the hydrates of calcium oxalate (adapted from [3] and thermal data from [138], [139] and [151]).

The thermal behavior of synthetic oxamite, $(NH_4)_2(C_2O_4)\cdot H_2O$, has so far been scarcely investigated. In an older TG-DTA study of this salt, it is stated that water loss begins above 70 °C with maximal rate at 115 °C. The anhydrous oxalate presents constant weight between 120 and 200 °C and above this temperature it decomposes in two steps, related to strong exothermic DTA signals at 235 and 300 °C, with liberation of CO, CO_2, water ammonia and formic acid and, apparently, with the intermediate formation of oxamide, $H_2N–CO–CO–NH_2$ [153].

The thermal behavior of the $M^{II}(C_2O_4)\cdot 2H_2O$ transition metal oxalates has also been often investigated, although in much of the published studies it is usually not clearly emphasized which of the crystal modifications (α-$M^{II}(C_2O_4)\cdot 2H_2O$ or β-$M^{II}(C_2O_4)\cdot 2H_2O$) were investigated.

As shown in section 5.1, the thermal degradation of humboldtine appears as relatively complex, a fact which was also observed in the case of synthetic $Fe^{II}(C_2O_4)\cdot 2H_2O$ samples degraded thermally under different experimental conditions. The importance of the atmosphere on the nature of the decomposition products has been pointed out even in earlier studies [154, 155] and confirmed also by most recent ones [146]. In a N_2 atmosphere, the main solid residue is Fe_2O_3 with the additional presence of a minor quantity of Fe_3O_4; in a H_2 atmosphere the major residue is elemental Fe with small contributions of Fe_2O_3 and Fe_3O_4; and in air Fe_2O_3 is again the main residue with the presence of small quantities of Fe_3O_4 and elemental Fe [146].

In another recent and very interesting thermogravimetric study, the decomposition of $Fe^{II}(C_2O_4)\cdot 2H_2O$ was investigated in the presence of the gaseous products generated during the reaction (CO, CO_2, and H_2O) and the formed solid phases were identified and characterized by ^{57}Fe-Mössbauer spectroscopy and X-ray diffraction [156]. On the basis of the obtained experimental results, a five-step decomposition mechanism for this oxalate in the atmosphere of its conversion gasses was proposed:

Step I: release of crystal water in the temperature range 170–230 °C:

$$Fe^{II}(C_2O_4)\cdot 2H_2O \longrightarrow Fe^{II}(C_2O_4) + 2H_2O$$

Step II: thermally induced conversion of the anhydrous oxalate to magnetite and carbon oxides at temperatures above 230 °C:

$$3Fe(C_2O_4) \longrightarrow Fe_3O_4 + 4CO + 2CO_2$$

Step III: reduction of the anhydrous oxalate by CO to Fe_3C, at temperatures above 360 °C:

$$3Fe(C_2O_4) + 2CO \longrightarrow Fe_3C + 7CO_2$$

Step IV: thermal conversion of the carbide, in the temperature range 415–535 °C:

$$Fe_3C \longrightarrow 3Fe + C$$

Step V: thermally induced reduction of magnetite to FeO by CO, at temperatures above 535 °C:

$$Fe_3O_4 + CO \longrightarrow 3FeO + CO_2$$

Furthermore, all these processes show the complexity and the different chemical pathways which may be involved in the thermal degradation of $Fe^{II}(C_2O_4)\cdot 2H_2O$ and the important effect of the atmospheres in which reactions take place.

Hydrated ferric oxalate has also been investigated many times by different authors, showing a relatively complex decomposition scheme [157]. In the first thermolysis step, the dehydration is, apparently, overlapped with the decomposition to ferrous oxalate and CO_2 liberation, generating a small residue of undecomposed ferric oxalate [131]. However, under oxidative conditions, the decomposition is far more straightforward generating α-Fe_2O_3 as the final decomposition product [158]. In the most detailed study on this system so far performed [157], the intermediate formation of $Fe(C_2O_4)$ was clearly proven in both, inert and oxidative, atmospheres. Moreover, the amount detectable of this intermediate under oxidative conditions clearly depends on the access of oxygen to the sample volume. Under a dynamic inert atmosphere, the decomposition takes place up to 210 °C and a small amount of Fe_3O_4 is also generated:

$$Fe_2(C_2O_4)_3 \longrightarrow 2Fe(C_2O_4) + 2CO_2$$

$$3Fe_2(C_2O_4)_3 \longrightarrow 2Fe_3O_4 + 10CO_2 + 8CO$$

Simultaneously, the dehydration process proceeds up to 300 °C. On the temperature range 300–390 °C, the decomposition of the initially generated ferrous oxalate takes place:

$$Fe(C_2O_4) \longrightarrow FeO + CO + CO_2$$

And the thermally unstable FeO undergoes disproportionation at temperatures below 570 °C:

$$4FeO \longrightarrow Fe_3O_4 + Fe$$

Above this temperature, the reverse process of synproportionation takes place:

$$Fe + Fe_3O_4 \longrightarrow 4FeO$$

Finally, it was confirmed that Fe_2O_3 is the final product under dynamic oxidative conditions.

The thermal decomposition of $Zn(C_2O_4)\cdot 2H_2O$ is much more simple, as in all atmospheres only the generation of ZnO, with concomitant CO and CO_2 liberation, is observed [146, 159]. Also in the case of $Ni(C_2O_4)\cdot 2H_2O$, NiO is obtained working in air or in N_2 atmosphere, whereas metallic Ni is generated in He or H_2 atmospheres [146, 160, 161]. Interestingly, dehydration of $Ni(C_2O_4)\cdot 2H_2O$ is never complete and water remains occluded in the partially dehydrated and very porous structure [160].

Cobalt oxalate, $Co(C_2O_4)\cdot 2H_2O$, generates Co_3O_4 in air and N_2 atmospheres and metallic Co in H_2 atmosphere [146] and also in He or He/H_2 atmospheres [162]. On the other hand, $[Co(C_2O_4)(H_2O)]\cdot 2H_2O$ releases water in two steps, lattice water in the temperature range 40–70 °C and coordinated water in the range 160–200 °C. The anhydrous oxalate is stable up to 280 °C and finally leads to Co_3O_4 [93].

Interesting differences are observed comparing the thermal behavior of α-$Mn(C_2O_4)\cdot 2H_2O$ and $Mn(C_2O_4)\cdot 3H_2O$ in air. For the dihydrate, the dehydration starts at about 130 °C and occurs in a unique step. For the trihydrate, water loss begins at lower temperature (about 80 °C) but in a three-step process [163]. The final decomposition of the anhydrous oxalates leads to the intermediate formation of Mn(III) and Mn(IV) species and the oxidation process is relatively weaker when starting with $Mn(C_2O_4)\cdot 3H_2O$. This fact implies that this crystal lattice stabilizes the lower oxidation states of manganese. The final annealing of $Mn(C_2O_4)\cdot 2H_2O$ at 450 °C leads to its complete transformation into Mn_3O_4. At the same temperature the trihydrate gives not only Mn_3O_4 but also an important quantity of Mn_2O_3 [163].

The thermal decomposition of copper(II) oxalate seems relatively complex as it is strongly dependent on the atmosphere in which decomposition is performed [87, 146, 164]. The retained zeolitic-type water is lost in the temperature range between 40 and 185 °C in air [87]. In this atmosphere, CuO is generated as the final decomposition product [146, 164], eventually with the intermediate formation of metallic Cu and Cu_2O [87]. In Ar or N_2 atmospheres, the final residue is mainly metallic Cu with small amounts of Cu_2O and, under certain conditions, traces of CuO [146, 164]:

$$Cu(C_2O_4) \longrightarrow Cu + 2CO_2$$

$$2Cu(C_2O_4) \longrightarrow Cu_2O + CO + 3CO_2$$

$$Cu(C_2O_4) \longrightarrow CuO + CO + CO_2$$

Some oxidation of elemental Cu can also occur due to the presence of residual air in the experimental arrangement or by CO_2 disproportionation [164].

Totally pure Cu can only by obtained under a H_2 atmosphere [146].

In the case of the trihydrated cadmium oxalate, $CdC_2O_4\cdot 3H_2O$, dehydration occurs in a single step in the temperature range 31–179 °C. At about 340 °C, $CdCO_3$ is generated and, finally, at temperatures above 700 °C, CdO remains as the final decomposition product [97]. Notwithstanding, under certain experimental conditions it is also possible to obtain metallic Cd as the final decomposition product [165].

For the most complex oxalates only synthetic wheatleyite, $Na_2Cu(C_2O_4)_2\cdot 2H_2O$, has been investigated in detail [166]. In a flowing N_2-atmosphere, the elimination of water

occurs in three consecutive steps at 78, 100, and 111 C. The anhydrous complex transforms to a mixture of $CuCO_3$ and Na_2CO_3 with liberation of CO, at 255 °C; whereas, at 349 °C the carbonates are converted to the respective oxides with CO_2 liberation.

The thermal behavior of synthetic minguzzite, $K_3Fe^{III}(C_2O_4)_3{\cdot}3H_2O$, has often been investigated. Water is lost immediately on heating and is complete at 160 °C (in air or N_2 atmosphere) [158]. This process was reinvestigated in detail most recently [167]. The generated anhydrous $K_3[Fe(C_2O_4)_3]$ is stable up to 260 °C and above this temperature Fe_2O_3 and $K_2C_2O_4$ are generated in air. Above 330 °C, decomposition of the potassium oxalate to K_2CO_3 takes place, generating a stable residue at 380 °C. Finally, at 580 °C another small weight loss related to the formation of $KFeO_2$ is observed [158]. In N_2 atmosphere, the final residue obtained at about 500 °C is a mixture of K_2CO_3 and elemental iron. Different speculations about the possible degradation mechanism under this atmosphere were advanced, the most probable may be a initial reduction of Fe(III) to Fe(II) according to:

$$2K_3[Fe(C_2O_4)_3] \longrightarrow 2K_2[Fe(C_2O_4)_2] + K_2C_2O_4 + 2CO_2$$

and the subsequent degradation of the Fe(II) complex into a mixture of $Fe_3O_4/K_2C_2O_4$. The final reaction involves the reduction of the oxide by the CO generated in the decomposition of $K_2C_2O_4$ ($K_2C_2O_4 \rightarrow K_2CO_3 + CO$) [158]. A somewhat different mechanism was postulated most recently [168].

The related Al(III) complex, $K_3[Al(C_2O_4)_3]{\cdot}3H_2O$, which may be of interest in relation to the thermal behavior of zhemchuzhnikovite, has also been repeatedly investigated [168, 169].

In addition, the thermal decomposition of the analogous ammonium compound, $(NH_4)_3[Fe^{III}(C_2O_4)_3]{\cdot}3H_2O$, is well known and has been investigated by TG/DTA measurements in air [170] and N_2 [158]. In air, the first stage of decomposition starts at about 100 °C and corresponds to the evolution of the three water molecules. This dehydration is followed by a second stage in which the sample ignites at around 260 °C and burns rapidly, generating finely divided Fe_2O_3 [170]. In N_2 atmosphere, the final products are a mixture of Fe, Fe_3O_4, and FeO [158].

6. Spectroscopic and magnetic properties

6.1. *Vibrational spectra*

Infrared and Raman spectra of oxalate salts and oxalato complexes have been widely investigated and different general assignment proposals have been advanced [171–176]. Nevertheless, systematic vibrational spectroscopic studies of natural oxalates remain relatively scarce. Only recently, detailed Raman studies have been performed for the mineral species whewellite, weddellite, natroxalate, oxamite, moolooite, humboldtine, and glushinskite [177, 178].

On the other hand, it has been shown that vibrational spectroscopy is a very useful and powerful tool for the investigation of biominerals in plants and related systems [179]. As an example, figure 6 shows the FTIR spectra of whewellite and weddellite samples isolated from two cactaceae species [180] and, as it can be seen, both biominerals can be clearly and unambiguously differentiated by this methodology. In the last years, IR and Raman spectroscopy have often been used for such type of studies in different plant species [45, 179–187].

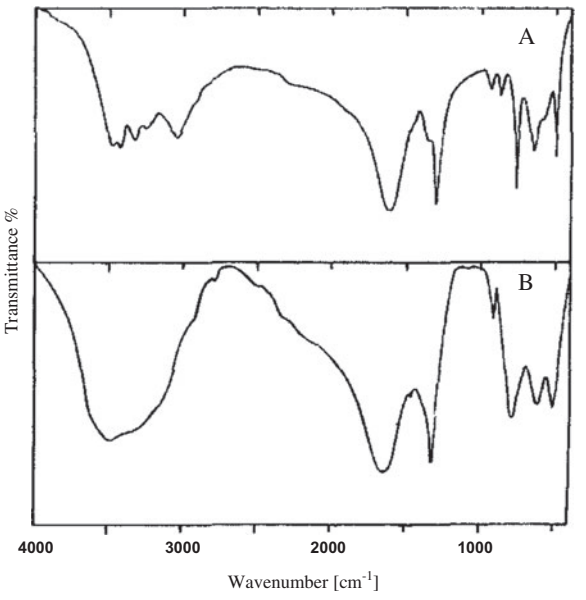

Figure 6. Infrared spectra of whewellite from the cactaceae *Opuntia longispina* (A) and weddellite from the cactaceae *Pyrrhocactus strausianus* (B) (taken from the study of Ref. [180]).

Other natural oxalates frequently investigated by means of IR and/or Raman spectroscopy were urinary stones (cf. e.g. [188–194]).

Concerning the synthetic oxalates analogous to the natural ones, some of them have been investigated much time ago, but the spectra of an important number, especially those containing transition metal cations have only been recorded and interpreted in recent years.

The IR and Raman spectra of solid $Na_2(C_2O_4)$ were investigated in comparison with those of the analogous lithium and potassium salts [195], whereas the vibrational spectra of all alkaline oxalates in aqueous solution were also investigated in great detail, including concentration effects in the analyzed solutions [176].

A first assignment of the IR and Raman spectra of synthetic oxamite, $(NH_4)_2(C_2O_4)\cdot H_2O$, was performed at 298 and 10 K, using a single monocrystal of the oxalate [196]. Most recently, the Raman spectra of the powdered solid were reinvestigated, including measurements with the isotopomeric species $(NH_4)_2(^{12}C_2O_4)\cdot H_2O$ and $(NH_4)_2(^{13}C_2O_4)\cdot H_2O$, and discussed in detail in comparison with those of the analogous potassium salt and on the basis of force field calculations [197].

In the case of the calcium oxalates, very few studies have been performed with synthetic samples. Most of the available information was derived from the mentioned studies of natural samples obtained from the mineral and vegetal kingdom or from clinical studies. Notwithstanding, some specific studies can be mentioned. The IR spectrum of $Ca(C_2O_4)\cdot H_2O$ and its deuterated analogous, $Ca(C_2O_4)\cdot D_2O$ [198] as well as the IR and Raman spectra of the same monohydrate and its dehydration product [199] were investigated much time ago. Raman spectra of both the monohydrate and the dihydrate were also reported [200]. Moreover, a detailed assignment of the IR spectra of the mono-, di-, and tri-hydrate is known, including an analysis of the main spectral differences between the three hydrates [53].

Finally, in a most recent study, the IR spectrum of a crystalline sample of $Ca(C_2O_4)\cdot H_2O$, obtained by the gel method, was recorded and briefly discussed [201].

The analysis of the IR and Raman spectra of the magnesium oxalates, showed practically identical spectra for the α-$Mg(C_2O_4)\cdot 2H_2O$ and β-$Mg(C_2O_4)\cdot 2H_2O$ modifications, confirming the strong structural similarities between them [202]. The same behavior was observed in the case of the other *α*/*β* pairs of metallic oxalates that shall be discussed in the following paragraphs. As an example of the spectral pattern of these complexes, figure 7 shows the IR and Raman spectra of α-$Mg(C_2O_4)\cdot 2H_2O$ in the spectral range between 2000 and 400 cm^{-1}, whereas the corresponding assignment is presented in table 5 [202]. IR spectra of partially deuterated samples of this complex were also analyzed in order to attain a better insight into the possible origin of some of the lower energy bands. This analysis confirms that the medium intensity of the IR band located at 690 cm^{-1} is effectively related to a librational mode of the H_2O molecules [202].

In the case of magnesium oxalate, also the spectra of the anhydrous complex were thoroughly investigated. These spectra are much simple than those of the two hydrated forms but the spectral analysis clearly confirms that also after dehydration the complex retains the typical chain structure shown in figure 1 [202].

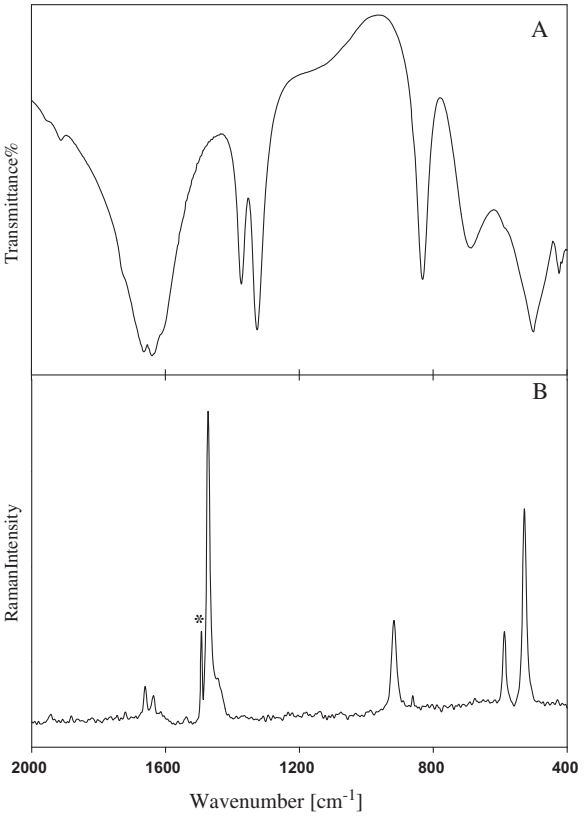

Figure 7. FTIR (A) and FT-Raman spectra (B) of α-$Mg(C_2O_4)\cdot 2H_2O$ in the spectral range between 2000 and 400 cm^{-1} (adapted from Ref. [202]).

Table 5. Assignment of the vibrational spectra of α-$Mg(C_2O_4)\cdot 2H_2O$ (band positions in cm^{-1}) [202].

Infrared	Raman	Assignment
3385vs, br	3370m	ν(OH) (H_2O)
3233w, 3130w		
1663sh	1661w	
1640vs	1635vw	ν_{as}(C–O)
	1615vw	
	1473vs	ν_s(C–O) + ν(C–C)
	1450vw	ν_s(C–O) + δ(OCO)
1372s/1324vs		ν_s(C–O) + δ(OCO)
	1412m*	Instrumental noise
	1160vw	
	918m	ν(C–C)
	870vw	
830vs		ν(C–C) + δ(OCO)
690m		ρ(H_2O)
	588m	δ_{ring}
	528s	δ_{ring}
501s		δ_{ring}
421m		ν(Mg–O) (?)

Note: vs, very strong; s, strong; m, medium; w, weak; vw, very weak; sh, shoulder; br, broad.
*Signifies the band marked with (*) in the Raman spectrum of Figure 7.

The three hydrates of Mn(II) oxalate, α-$Mn(C_2O_2)\cdot 2H_2O$, γ-$Mn(C_2O_2)\cdot 2H_2O$, and Mn $(C_2O_2)\cdot 3H_2O$, have also been recently investigated by IR and Raman spectroscopy [203]. Interestingly, and despite their structural differences, commented in section 4.1.4, the vibrational spectra of the three complexes are practically comparable in the spectral range between 2000 and 400 cm^{-1}, showing only minor intensity differences in some of the bands. However, important spectral differences are observed in the higher energy region (4000–2500 cm^{-1}) in which the O–H stretching modes of the water molecules are located. Therefore, the spectral analysis of this higher energy region allows an easy differentiation of the three hydrates [203].

Also, the two modifications of the dihydrated Fe(II) oxalate show practically identical IR and Raman spectral patterns [132]. The Raman spectrum of α-$Fe(C_2O_4)\cdot 2H_2O$ resembles closely that of natural humboldtine [177, 178]. As mentioned in section 4.1.6, the IR and Raman spectra of the most simple Fe(III) oxalate, $Fe_2(C_2O_4)_3\cdot 4H_2O$, were also recorded and assigned [132]. From the comparison of the IR and Raman spectra of single crystals of α-$Fe(C_2O_4)\cdot 2H_2O$ and α-$Mn(C_2O_4)\cdot 2H_2O$, it was possible to analyze some differences in the hydrogen bond geometries of both oxalates. In addition, the spectral characteristics of the ν(Fe–O) stretching band suggest a direct manifestation of the Jahn–Teller effect on the Fe(II) cation [83].

In another recent study, the vibrational spectra of the α-$M^{II}(C_2O_4)\cdot 2H_2O$ complexes (with M^{II} = Co, Ni, Zn), also structurally related to humboldtine, were investigated. As expected, their spectral patterns resemble closely those of the other previously mentioned α-M^{II}-$C_2O_4\cdot 2H_2O$ oxalates [204].

As expected from the close structural analogies, the vibrational spectra of synthetic mooolooite, $Cu(C_2O_4)\cdot 0.2H_2O$, are also very similar to those of the mentioned complexes [205]. The most striking difference with these complexes arises in the higher energy region, as the zeolitic water trapped in the lattice generates only a broad and relatively undefined IR-absorption at

about 3575 cm^{-1} with no Raman counterpart [205]. Besides, the Raman spectrum of the synthetic complex appears better defined than that of natural moolooite [177, 178].

IR and Raman spectra of synthetic wheatleyite, $Na_2Cu/C_2O_4)_2{\cdot}2H_2O$, were investigated but analyzed without the consideration of the known structural data [206]. Subsequently, the spectroscopic behavior of this complex was reinvestigated in comparison with the spectra of the stoichiometrically related but structurally different ammonium and potassium salts. The discussion of these spectra on the basis of their structural peculiarities, allowed to explain small differences between the two structural groups [207].

The IR spectrum of synthetic minguzzite, $K_3[Fe(C_2O_4)_3]{\cdot}3H_2O$, was recorded and discussed with the aid of a normal coordinate analysis in a classic article on oxalato metal complexes by Fujita *et al*. [172]. This article also presents results for similar complexes derived from other M(III) cations, including $K_3[Al(C_2O_4)_3]{\cdot}3H_2O$, certainly relevant for the species discussed in this review. It was also clearly established that most of the spectral bands are metal sensitive and that the frequencies of the uncoordinated C=O stretching bands increase, and those of the coordinated C–O stretching bands decrease, as the frequency of the metal–oxygen ν(M–O) stretching band increases. Besides, these M–O stretching bands are not very characteristic as they are coupled with ring vibrations of the chelating ligand.

6.2. *Electronic spectra*

The visible and ultraviolet absorption spectra of many of the known metal oxalates were investigated long ago in water as a solvent and, in some cases, in the presence of an excess of oxalate anion, to stabilize the complex under observation [49].

As the oxalato anion is located close to water in the spectrochemical series of ligands [208], one may expect a similar spectroscopic behavior of the aqua and oxalate complexes in solution.

Only few oxalato complexes have been investigated as solid dispersions by reflectance spectroscopy or in the crystalline state in a pure form or doped in inert matrixes.

One of the few known examples is the absorption of polarized light by single crystals of $NaMg[Al(C_2O_4)_3]{\cdot}9H_2O$, with part of Al(III) replaced by Fe(III), which allowed a detailed assignment of the observed electronic transitions of this cation. The estimated Dq crystal field parameter (1500 cm^{-1}) is similar to that of the aqua complex [126]. In the case of the anhydrous $K_3[Fe(C_2O_4)_3]$, the UV–vis–NIR spectrum exhibited two broad absorption bands at 644 and 924 nm, which were attributed to ligand-to-metal charge transfers [125].

For synthetic moolooite, $Cu(C_2O_4){\cdot}0.2H_2O$, the visible electronic reflectance spectrum presents a unique, very strong and broad band in the visible range, centered at about 760 nm and another very strong one at ca. 300 nm [205]. The visible band is assigned to the expected "d–d" transition and its position suggests that the Cu–O π-bonding is somewhat weaker in this oxalato complex than in the related and also planar bis-acetylacetonatocopper(II) complex [205, 209]. The higher energy band can be assigned to an intraligand-charge transfer transition [205, 210].

6.3. *Magnetic properties*

A characteristic feature of the crystal structures of all the $M^{II}(C_2O_4){\cdot}2H_2O$ systems with M^{II} = 3d transition element is the presence of linear chains of oxalate–metal groups running

along the *b* axis (cf. again figure 1), providing a relatively strong antiferromagnetic coupling of these 3d ions in the linear chains. Nearest-neighbor chains are linked together by relatively weak hydrogen bonds. Thus, these systems are expected to exhibit quasi 1-D magnetic behavior characterized by a significant correlation along the *b* axis at temperatures above the temperature of transition to a 3-D magnetic ordering [211, 212].

No information on the magnetic behavior of natural oxalates has so far been reported, but although magnetic measurements for synthetic oxalato complexes were repeatedly reported in the past [49], we would like to restrict this information only to some of the most recent studies in this field.

During the study of the thermal decomposition of α-$Mn(C_2O_4)\cdot 2H_2O$ and $Mn(C_2O_4)\cdot 3H_2O$, and in order to follow the magnetic behavior of the degradation products, magnetic susceptibility measurements in the temperature range 25–300 °C were performed. They show that both oxalates present an effective magnetic moment, μ_{eff}, equal to 5.92 Bohr magnetons and a Weiss temperature $\theta = -13$ K. The negative value of the Weiss constant confirms the antiferromagnetic behavior of these oxalates [163].

The magnetic structure of a polycrystalline sample of α-$Mn(C_2O_4)\cdot 2D_2O$ was investigated by neutron diffraction experiments in the temperature range between 1.5 and 295 K and by bulk magnetic susceptibility measurements (4.2–295 K). At temperatures above 80 K, the complex show a typical Curie–Weiss behavior with $S = 5/2$ and $\theta = -11.2$ K. On the other hand, the Néel temperature, T_N, lies at around 2.6 K and magnetic intra-chain interactions begin at around 10 K [212]. In the case of $[Mn(C_2O_4)(H_2O)_2]\cdot H_2O$, Curie–Weiss behavior is observed at temperatures above 30 K with $\theta = -20.36$ K. A Néel temperature of 2.82 K was determined by specific heat measurements. It was admitted that around 12 K 1-D intra-chain magnetic interactions occur and the long-range ordering below T_N is further developed by the mediating of interchain hydrogen bonds [90].

Also for α-$Fe(C_2O_4)\cdot 2D_2O$, the magnetic structure was investigated by neutron diffraction experiments in the temperature range between 4.2 and 300 K [213], complementing an earlier work on magnetic susceptibility measurements (1.3–300 K) on α-$Fe(C_2O_4)\cdot 2H_2O$ [214]. At temperatures above 80 K, the complex follows a Curie–Weiss law with $\theta = -25.4$ K [214], whereas the Néel temperature was found at 16 K [213].

The magnetic behavior of α-$Co(C_2O_4)\cdot 2H_2O$ has often been investigated, including neutron diffraction experiments with α-$Co(C_2O_4)\cdot 2D_2O$, in the temperature range from 1.4 to 293 K [215] and EPR measurements of Co(II) diluted in a $Zn(C_2O_4)\cdot 2H_2O$ matrix [216]. For this complex, the Néel temperature was determined, by heat capacity measurements, to lie at 6.2 K [216]. Interestingly, in this case also the magnetic behavior of the β-$Co(C_2O_4)\cdot 2H_2O$ modification has recently been investigated [217]. Above 100 K, the complex shows a typical Curie–Weiss behavior, with θ-values ranging between −31.8 and −40.7 K, for different investigated samples. The Néel temperature was found at about 7.5 K. Although the observed general magnetic behavior is totally consistent with the existence of antiferromagnetic ordering, the hysteresis measured in magnetization experiments as a function of the magnetic field reveals that the intra- and inter-chain magnetic interactions tilt the spins, distorting the antiferromagnetic order and producing a weak ferromagnetic behavior [217].

The related tetrahydrated cobalt(II) oxalate, $[Co(C_2O_4)(H_2O)_2]\cdot 2H_2O$, follows a Curie–Weiss law above 70 K, with $\theta = -68.8$ K and the magnetic susceptibility *vs.* temperature curve shows a maximum at about 26 K [93].

For $NiC_2O_4\cdot 2H_2O$, the magnetic behavior of both the α- and β-modifications were investigated. The α-$NiC_2O_4\cdot 2H_2O$, obtained in the form of nanorods, fits a Curie–Weiss law at

temperatures above 100 K with θ-values of −83.4 or −90.4 K, depending on the synthetic procedure employed in the preparation of the nanorods, and the susceptibility displayed a broad transition at about 40 K [218]. β-$NiC_2O_4{\cdot}2H_2O$ follows also a Curie–Weiss law at temperatures above 100 K with θ-values ranging between −76.9 and −99.8 K, values which are indicative of significant antiferromagnetic exchange interactions. Interestingly, in the temperature range between 3.3 and 43 K, a weak ferromagnetic behavior could be observed [219].

For the recently reported *cis*-$NiC_2O_4{\cdot}2H_2O$ form, a detailed analysis of the magnetic behavior was performed in the temperature range 2.5–255 K and some comparisons with the magnetic properties of the α-$NiC_2O_4{\cdot}2H_2O$ were made [94].

The magnetic behavior of $Cu(C_2O_4){\cdot}nH_2O$ has often been investigated, as a classical example of a linear chain of strongly antiferromagnetically coupled spin doublets [86, 88, 211, 220, 221]. EPR studies on this complex have also been performed, as a function of temperature and frequency [222].

In the case of $Na_2[Cu(C_2O_4)_2]{\cdot}2H_2O$, a weak antiferromagnetic coupling was observed, originated by interactions within the chains of stacked $[Cu(C_2O_4)_2]^{2-}$ units, as shown in figure 3(A) [115]. On the other hand, the stoichiometrically related complexes $K_2[Cu(C_2O_4)_2]{\cdot}2H_2O$ and $(NH_4)_2[Cu(C_2O_4)_2]{\cdot}2H_2O$ show a Curie–Weiss behavior with very small θ-values (0.7 K for the potassium salt and 0.6 K for the ammonium salt), whereas the EPR results suggest some magnetic interactions between the metallic centers [223], but the coupling is evidently weaker than in the sodium salt. This difference can clearly be related to the different structures of these compounds. As shown in figure 3(B), in the K- and NH_4-salts interactions occur between $[Cu(C_2O_4)_2]^{2-}$ and $[Cu(C_2O_4)_2(H_2O)_2]^{2-}$ units disposed in such a way that the interactions take place through very weak oxalate bridges over distances of more than 5 Å, whereas in the Na salt, the structural arrangement allows for direct δ-type overlapping of the magnetic orbitals [115].

For synthetic minguzzite, $K_3[Fe(C_2O_4)_3]{\cdot}3H_2O$, magnetic susceptibility was measured between 80 and 300 K, showing a Curie–Weiss behavior with $\theta = -3.0$ K, suggesting only weak magnetic interactions between the Fe(III) centers in this structure [224]. In an older magnetic study of this complex, the anisotropy of the $^6A_{1g}$ ground state was detected by magnetic susceptibility measurements of the crystalline material, for the first time [225]. Furthermore, the EPR spectra for powdered polycrystalline samples of this complex have been determined at both X- and Q-band frequencies in the temperature range between 77 and 300 K [226] For the related anhydrous complex, $K_3[Fe(C_2O_4)_3]$, the X-band ESR spectrum at room temperature shows similar features [125] as those reported for its trihydrated counterpart [226]. Besides, the variation of induced magnetic moment with respect to the applied magnetic field shows that the intensity of magnetization varies linearly with the applied field, supporting the paramagnetic nature of this complex at room temperature [125].

6.4. *Mössbauer spectra of iron oxalates*

^{57}Fe-Mösbauer spectra of the iron (II) oxalates have been repeatedly measured [227–230], including a low temperature analysis (4.2 K) of the hyperfine Zeeman splitting [231].

In the most recent study, it was shown that both α-$Fe(C_2O_4){\cdot}2H_2O$ and β-$Fe(C_2O_4){\cdot}2H_2O$ practically present the same hyperfine parameters ($\delta = 1.20(1)$ and $\Delta Q = 1.73(1)$ mm/sec, referred to α-Fe, at 298 K), which make it impossible to differentiate these two

crystalline modifications even by this experimental technique [132]. The measured parameters are in agreement with the presence of an octahedral or quasi-octahedral environment of the Fe(II) center, with a high-spin electronic configuration [132].

Interestingly, after dehydration and generation of the anhydrous oxalate, only a small increase in the ΔQ-value is observed [156].

In the case of $Fe_2(C_2O_4)_3 \cdot 4H_2O$, the presence of a unique quadrupole doublet of narrow line width clearly confirms the structural equivalency of both Fe(III) ions. The observed isomer shift ($\delta = 0.38(1)$ mm/sec) lies in the range expected for an octahedral FeO_6 environment. Besides, the relatively low quadrupole splitting ($\Delta Q = 0.39(1)$ mm/sec), which is appreciably lower than those found in mixed ligand Fe(III) oxalato complexes [230], indicates the presence of a scarcely distorted octahedral environment and a high-spin electronic configuration for Fe(III) [132].

For the $K_3[Fe(C_2O_4)_3] \cdot 3H_2O$ complex, the Mössbauer spectra present only a single and relatively broad peak without quadrupolar splitting [232–234], suggesting the presence of a relatively regular and scarcely distorted octahedral environment around the high-spin Fe(III) center. Values measured for the isomer shift were $\delta = 0.44(2)$ mm/sec (at 77 K) and $\delta = 0.33(2)$ mm/s (at 293 K) [233].

Acknowledgements

The continuous support from the Universidad Nacional de La Plata to our work is gratefully acknowledged. The author is also indebted to the colleagues and coworkers which names appear in the references.

References

[1] H. Strunz. *Mineralogische Tabellen*, 7th Edn, pp. 494–495, Geest & Portig, Leipzig (1978).
[2] S. Weiner, P.M. Dove. In *Reviews in Mineralogy and Geochemistry*, P.M. Dove, J.J. De Yoreo, S. Weiner (Eds.), Vol. 54, pp. 1–29, Mineralogical Soc. America/Geochemical Soc., Washington, DC (2003).
[3] T. Echigo, M. Kimata. *Can. Mineral.*, **48**, 1329 (2010).
[4] J.J.R. Fraústo da Silva, R.J.P. Williams. *The Biological Chemistry of the Elements*, pp. 467–494, Clarendon Press, Oxford (1991).
[5] E.J. Baran. *Química Bioinorgánica* [Bioinorganic Chemistry], pp. 197–212, McGraw Hill Interamericana de España S.A., Madrid (1995).
[6] E.J. Baran, P.V. Monje. In *Biomineralization. From Nature to Application, Metal Ions in Life Sciences*, A. Sigel, H. Sigel, R.K.O. Sigel (Eds.), Vol. 4, pp. 219–254, Wiley, Chichester (2008).
[7] P.A. Nakata. *Plant Sci.*, **164**, 901 (2003).
[8] V.R. Franceschi, P.A. Nakata. *Ann. Rev. Plant Biol.*, **56**, 41 (2005).
[9] P.V. Monje, E.J. Baran. In *Advances in Plant Physiology*, A. Hemantaranjan (Ed.), Vol. 7, pp. 395–410, Scientific Publishers, Jodhpur (2004).
[10] F.R. Ahmed, D.W.J. Cruickshank. *Acta Crystallogr.*, **6**, 385 (1953).
[11] E.D. Stevens, P. Coppens. *Acta Crystallogr., Sect. B: Struct. Crystallogr. Cryst. Chem.*, **36**, 1864 (1980).
[12] A.E. Martell, R.M. Smith (Eds.). *Critical Stability Constants*, Vol. 3, pp. 92–95, Plenum Press, New York (1977).
[13] F.A. Cotton, G. Wilkinson, C.A. Murillo, M. Bochmann. *Advanced Inorganic Chemistry*, 6th Edn, pp. 484–488, Wiley, New York (1999).
[14] V.N. Serezhkin, Yu. Artem'eva, L.B. Serezhkina, Yu.N. Mikhailov. *Russ. J. Inorg. Chem.*, **50**, 1019 (2005).
[15] B.A. Hofmann, S.M. Bernasconi. *Chem. Geol.*, **149**, 127 (1998).
[16] G.L. Gardner. *J. Cryst. Growth*, **30**, 158 (1975).
[17] G.H. Nancollas. In *Biological Mineralization and Demineralization*, G.H. Nancollas (Ed.), pp. 79–99, Springer Verlag, Berlin (1982).
[18] F.A. Bannister, M.H. Hey. *Discov. Rep.*, **13**, 60 (1936).

[19] R.A Young, W.E. Brown. In *Biological Mineralization and Demineralization*, G.H. Nancollas (Ed.), pp. 101–141, Springer Verlag, Berlin (1982).
[20] R. Basso, G. Lucchetti, L. Zefiro, A. Palenzona. *N. Jahrb. Mineral. Monatsh.*, 84 (1997).
[21] J.L. Jambor, E.S. Grew, A.C. Roberts. *Am. Mineral.*, **83**, 185 (1998).
[22] N.V. Chukanov, D.I. Belakovskiy, R.K. Rastsvetaeva, O.V. Karimova, A.E. Zadov. *Zap. Vser. Min. Ob.*, **130**, 32 (2001).
[23] R.K. Rastsvetaeva, N.V. Chukanov, Yu.V. Nekrasov. *Dokl. Chem.*, **381**, 329 (2001).
[24] J.L. Jambor, M.K. Pertsev, A.C. Roberts. *Am. Mineral.*, **82**, 430 (1997).
[25] H. Winchell, R.J. Benoit. *Am. Mineral.*, **36**, 590 (1951).
[26] C. Garavelli. *Rend. Soc. Ital. Mineral. Petrol.*, **11**, 176 (1955).
[27] D. Atencio, J.M.N. Coutinho, S. Graeser, P.A. Matioli, L.A.D. Menezes Filho. *Am. Mineral.*, **89**, 1087 (2004).
[28] R.M. Clarke, J.R. Williams. *Mineral. Mag.*, **50**, 295 (1986).
[29] R.C. Rouse, D.R. Peacor, P.J. Dunn, W.B. Simmons, D. Newbury. *Am. Mineral.*, **71**, 1240 (1986).
[30] M. Fleischer. *Am. Mineral.*, **47**, 1482 (1962).
[31] C.L. Garavelli. *Atti Accad. Naz. Lincei, Cl. Sci. Fis. Mat. Nat. Rend.*, **18**, 392 (1955).
[32] M. Fleischer. *Am. Mineral.*, **41**, 370 (1956).
[33] D.R. Peacor, R.C. Rouse, E.J. Essene, R.J. Lauf. *Can. Mineral.*, **37**, 1453 (1999).
[34] R. Rouse, D.R. Peacor, E.J. Essene, T.D. Coskren, R.J. Lauf. *Geochim. Cosmochim. Acta*, **65**, 1101 (2001).
[35] N. Chukanov, I. Pekov, L. Olysych, W. Massa, O. Yakubovich, A. Zadov, R. Rastsvetaeva, M. Vigasina. *Geol. Ore Deposits*, **52**, 778 (2010).
[36] H.T. Horner, B.L. Wagner. In *Calcium Oxalate in Biological Systems*, S.R. Khan (Ed.), pp. 53–72, CRC Press, Boca Raton, FL (1995).
[37] H.J. Arnott. In *Calcium Oxalate in Biological Systems*, S.R. Khan (Ed.), pp. 73–111, CRC Press, Boca Raton, FL (1995).
[38] C. Ascaso, J. Galván, C. Rodríguez-Pascual. *Pedobiologia*, **24**, 219 (1982).
[39] J. Chen, H.P. Blume, L. Beyer. *Catena*, **39**, 121 (2000).
[40] P. Adamo, F. Violante. *Appl. Clay Sci.*, **16**, 229 (2000).
[41] M.J. Wilson, D. Jones. *Pedobiologia*, **26**, 373 (1984).
[42] J.E. Chisholm, G.C. Jones, O.W. Purvis. *Mineral. Mag.*, **51**, 715 (1987).
[43] G.M. Gadd. *Adv. Microb. Physiol.*, **41**, 47 (1999).
[44] M.J. Wilson, D. Jones, J.D. Russell. *Mineral. Mag.*, **43**, 837 (1980).
[45] P.V. Monje, E.J. Baran. *Phytochemistry*, **66**, 611 (2005).
[46] K. Kawamura, I.R. Kaplan. *Geochim. Cosmochim. Acta*, **51**, 3201 (1987).
[47] E.J. Baran. In *Advances in Plant Physiology*, A. Hemantaranjan (Ed.), Vol. 12, pp. 369–389, Scientific Publishers, Jodhpur (2011).
[48] D. Svedružić, S. Jónsson, C.G. Toyota, L.A. Reinhardt, S. Ricagno, Y. Lindqvist, N.G.J. Richards. *Arch. Biochem. Biophys.*, **433**, 176 (2005).
[49] K.Y. Krishnamurty, G.M. Harris. *Chem. Rev.*, **61**, 213 (1961).
[50] G.A. Jeffrey, G.E. Parry. *J. Am. Chem. Soc.*, **76**, 5283 (1954).
[51] D.A. Reed, M.M. Olmstead. *Acta Crystallogr., Sect. B: Struct. Crystallogr. Cryst. Chem.*, **37**, 938 (1981).
[52] R.E. Dinnebier, S. Vensky, M. Panthöfer, M. Jansen. *Inorg. Chem.*, **42**, 1499 (2003).
[53] V. Babić-Ivančić, H. Füredi-Milhofer, B. Purgarić, N. Brničević, Z. Despotović. *J. Cryst. Growth*, **71**, 655 (1985).
[54] F. Grases, A. Millan, A. Conte. *Urol. Res.*, **18**, 17 (1990).
[55] A. Millan. *Cryst. Growth Des.*, **1**, 245 (2001).
[56] E.V. Petrova, N.V. Gvodzdev, L.N. Rashkovich. *J. Optoelectron. Adv. Mater.*, **6**, 261 (2004).
[57] S. Deganello, O.E. Piro. *N. Jahrb. Mineral. Monatsh.*, 81 (1981).
[58] S. Deganello. *Z. Kristallogr.*, **152**, 247 (1980).
[59] V. Tazzoli, C. Domeneghetti. *Am. Mineral.*, **63**, 327 (1980).
[60] S. Deganello, A.R. Kampf, P.B. Moore. *Am. Mineral.*, **66**, 859 (1981).
[61] O. Hochrein, A. Thomas, R. Kniep. *Z. Anorg. Allg. Chem.*, **634**, 1826 (2008).
[62] F.T. Jones, L.M. White. *J. Am. Chem. Soc.*, **68**, 1339 (1946).
[63] A.N. Christensen. *Acta Chem. Scand.*, **46**, 240 (1992).
[64] L. Walter-Levy, J. Laniepce. *Compt. Rend. Acad. Sci. Paris*, **261**, 3789 (1965).
[65] A.N. Christensen, R. Hazell, I.C. Madsen. *Acta Crystallogr., Sect. B: Struct. Sci.*, **58**, 808 (2002).
[66] C. Sterling. *Nature*, **205**, 588 (1965).
[67] A.N. Christensen, R.G. Hazell. *Acta Chem. Scand.*, **52**, 508 (1998).
[68] D.J. Price, A.K. Powell, P.T. Wood. *Polyhedron*, **18**, 2499 (1999).
[69] D. Dollimore, J.L. Konieczay. *Thermochim. Acta*, **318**, 155 (1998).
[70] P. Barbaro, F. Cecconi, C.A. Ghilardi, S. Midollini, A. Orlandini, L. Alderighi, D. Peters, A. Vacca, E. Chinea, A. Mederos. *Inorg. Chim. Acta*, **262**, 187 (1997).
[71] S. Hendricks, M.E. Jefferson. *J. Chem. Phys.*, **4**, 102 (1936).

[72] G.A. Jeffrey, G.S. Parry. *J. Chem. Soc.*, 4864 (1952).
[73] J.H. Robertson. *Acta Crystallogr.*, **18**, 410 (1965).
[74] J.C. Taylor, T.M. Sabine. *Acta Crystallogr., Sect. B: Struct. Crystallogr. Cryst .Chem*, **28**, 3340 (1972).
[75] J.H. Robertson. *Acta Crystallogr.*, **18**, 417 (1965).
[76] R. Deyrieux, A. Péneloux. *Bull. Soc. Chim. Fr.*, 2675 (1969).
[77] R. Deyrieux, C. Berro, A. Péneloux. *Bull. Soc. Chim. Fr.*, 25 (1973).
[78] J.-P. Lagier, H. Pezerat, J. Dubernat. *Rev. Chim. Minér.*, **6**, 1081 (1969).
[79] A. Huizing, H.A.M. van Hal, W. Kwestroo, C. Langereis, P. Van Loosdregt. *Mater. Res. Bull.*, **12**, 605 (1977).
[80] L. Walter Levy, J. Perrotey. *Bull. Soc. Chim. Fr.*, 1697 (1970).
[81] L. Walter Levy, J. Perrotey, J.W. Visser. *Bull. Soc. Chim. Fr.*, 757 (1971).
[82] J. Soleimannejad, H. Aghabozorg, S. Hooshmand, M. Ghadermazi, J.A. Gharamaleki. *Acta Crystallogr.*, **E63**, m2389 (2007).
[83] T. Echigo, M. Kimata. *Phys. Chem. Miner.*, **35**, 467 (2008).
[84] J. Bacsa, D. Eve, K.R. Dunbar. *Acta Crystallogr.*, **C61**, m58 (2005).
[85] X.A. Chen, F.P. Song, X.A. Chang, H.G. Zang, W.Q. Xiao. *Acta Crystallogr.*, **E64**, m863 (2008).
[86] B.N. Figgis, D.J. Martin. *Inorg. Chem.*, **5**, 100 (1966).
[87] B. Donkova, D. Mehandjiev. *J. Mater. Sci.*, **40**, 3881 (2005).
[88] A. Michalowicz, J.J. Girerd, J. Goulon. *Inorg. Chem.*, **18**, 3094 (1979).
[89] Z.A.D. Lethbridge, A.F. Congreve, E. Esslemont, A.M.Z. Slawin, P. Lightfoot. *J. Solid State Chem.*, **172**, 212 (2003).
[90] W.Y. Wu, Y. Song, Y.Z. Li, X.Z. You. *Inorg. Chem. Commun.*, **8**, 732 (2005).
[91] X. Fu, C. Wang, M. Li. *Acta Crystallogr.*, **E61**, m1348 (2005).
[92] E. Wisgerhof, J.W. Geus. *Mater. Res. Bull.*, **18**, 993 (1983).
[93] U. García-Couceiro, O. Castillo, A. Luque, G. Beobide, P. Román. *Inorg. Chim. Acta*, **357**, 339 (2004).
[94] V. Paredes-García, I. Rojas, D. Venegas-Yazigi, E. Spodine, J.A.L.C. Resende, M.G.F. Vaz, M.A. Novak. *Polyhedron*, **30**, 3171 (2011).
[95] M. Molinier, D.J. Price, P.J. Wood, A.K. Powell. *J. Chem. Soc., Dalton Trans.*, 4061 (1997).
[96] G. Gavris, M. Stoia, O. Stanasel, S. Hodisan. *Chem. Bull. "Politehnika", Univ. Timisoara*, **55**, 143 (2010).
[97] A.M.E. Raj, D.D. Jayanthi, V.B. Jothy, M. Jayachandran, C. Sanjeeviraja. *Inorg. Chim. Acta*, **362**, 1535 (2009).
[98] H.S. Hua, W. Ru-Ji, C.W. Mak. *J. Crystallogr. Spectr. Res.*, **20**, 99 (1990).
[99] P. Orioli, B. Bruni, M. Di Vaira, L. Messori, F. Piccioli. *Inorg. Chem.*, **41**, 4312 (2002).
[100] A.V. Virovets, D.Y. Naumov, E.V. Boldyreva, N.V. Podberezskaya. *Acta Crystallogr.*, **C48**, 1882 (1993).
[101] A.N. Christensen, D.E. Cox, M.S. Lehmann. *Acta Chem. Scand.*, **43**, 19 (1989).
[102] N. Mancilla, M.C. D'Antonio, A.C. González-Baró, E.J. Baran. *J. Raman Spectrosc.*, **40**, 2050 (2009).
[103] O. Castillo, A. Luque, M. Julve, F. Lloret, P. Román. *Inorg. Chim. Acta*, **315**, 9 (2001).
[104] O. Castillo, A. Luque, P. Román, F. Lloret, M. Julve. *Inorg. Chem.*, **40**, 5526 (2001).
[105] J.Y. Lu, T.J. Schroeder, A.M. Babb, M. Olmstead. *Polyhedron*, **20**, 2445 (2001).
[106] X.R. Lin, R.Z. Ye, B.S. Liu, C.X. Wei, J.X. Chen. *Acta Crystallogr.*, **E62**, m2130 (2006).
[107] P.Z. Li, Q. Xu. *Acta Crystallogr.*, **E65**, m508 (2009).
[108] J. Wang, Y. Hou, Z. Fang. *Acta Crystallogr.*, **E66**, m1229 (2010).
[109] Y.D. Kondrashev, V.S. Bogdanov, S.S. Golubev, G.F. Pron. *J. Struct. Chem.*, **26**, 74 (1985).
[110] A. Koleżyński, A. Małecki. *J. Thermal Anal. Calorim.*, **96**, 645 (2009).
[111] E. Jeanneau, N. Audebrand, D. Louër. *Acta Crystallogr.*, **C57**, 1012 (2001).
[112] D. Palacios, A. Wladimirsky, M.C. D'Antonio, A.C. González-Baró, E.J. Baran. *Spectrochim. Acta, Part A*, **79**, 1145 (2011).
[113] U. Kolitsch. *Acta Crystallogr.*, **C60**, m129 (2004).
[114] W. Pannhorst, J. Löhn. *Z. Kristallogr.*, **139**, 236 (1974).
[115] A. Gleizes, F. Maury, J. Galy. *Inorg. Chem.*, **19**, 2074 (1980).
[116] T. Weichert, J. Löhn. *Z. Kristallogr.*, **139**, 223 (1974).
[117] M.A. Viswamitra. *J. Chem. Phys.*, **37**, 1408 (1962).
[118] W.G. Palmer. *Experimental Inorganic Chemistry*, Cambridge University Press, Cambridge (1954).
[119] R.C. Johnson. *J. Chem. Educ.*, **47**, 702 (1970).
[120] H.S. Booth (Ed.). *Inorganic Synthesis*, Vol. 1, p. 36., McGraw-Hill, New York (1939).
[121] J. Olmsted III. *J. Chem. Educ.*, **61**, 1098 (1984).
[122] P. Herpin. *Bull. Soc. Franç. Minéral. Cristallogr.*, **81**, 245 (1958).
[123] J.N. van Niekerk, F.R.L. Schoening. *Acta Crystallogr.*, **5**, 196 (1952).
[124] D. Taylor. *Aust. J. Chem.*, **31**, 1455 (1978).
[125] A. Saritha, B. Raju, M. Ramachary, Raghavaiah, K.A. Hussain. *Physica B*, **407**, 4208 (2012).
[126] T.S. Piper, R.L. Carlin. *J. Chem. Phys.*, **35**, 1809 (1961).
[127] L. Frossard. *Schweiz. Mineral. Petrog. Mitt.*, **36**, 1 (1956).
[128] T.S. Piper, R.L. Carlin. *J. Chem. Phys.*, **33**, 608 (1960).

[129] O.S. Mortensen. *J. Chem. Phys.*, **47**, 4215 (1967).
[130] M. Fleischer. *Am. Mineral.*, **49**, 439 (1964).
[131] A.K. Galwey, M.A. Mohamed. *Thermochim. Acta*, **213**, 279 (1993).
[132] M.C. D'Antonio, A. Wladimirsky, D. Palacios, L. Coggiolaa, A.C. González-Baró, E.J. Baran, R.C. Mercader. *J. Braz. Chem. Soc.*, **20**, 445 (2009).
[133] F.C. Hawthorne, S.V. Krivovichev, P.C. Burns. *Rev. Mineral. Geochem.*, **40**, 1 (2000).
[134] Y.P. Yuan, J.L. Song, J.G. Mao. *Inorg. Chem. Commun.*, **7**, 24 (2004).
[135] N. Wang, S.T. Yue, Y.L. Liu. *J. Coord. Chem.*, **62**, 1914 (2009).
[136] C.H. Banford, C.F.H. Tipper (Eds.). *Chemical Kinetics, Reactions in the Solid State*, Vol. 22, pp. 218–224, Elsevier, Amsterdam (1980).
[137] D. Dollimore. *Thermochim. Acta*, **117**, 331 (1987).
[138] R.L. Frost, M.L. Weier. *Thermochim. Acta*, **409**, 79 (2004).
[139] R.L. Frost, M.L. Weier. *Thermochim. Acta*, **406**, 221 (2003).
[140] R.L. Frost, K. Erickson, M. Weier. *J. Therm. Anal. Calorim.*, **77**, 851 (2004).
[141] R.L. Frost, M.L. Weier. *J. Therm. Anal. Calorim.*, **75**, 277 (2004).
[142] R.L. Frost, M. Adebajo, M.L. Weier. *Spectrochim. Acta, Part A*, **60**, 643 (2004).
[143] R.L. Frost, M.L. Weier. *N. Jahrb. Mineral. Monatsh.*, 27 (2004).
[144] B.V. L'vov. *Thermochim. Acta*, **364**, 99 (2000).
[145] V.V. Boldyrev. *Thermochim. Acta*, **388**, 63 (2002).
[146] M.A. Mohamed, A.K. Galwey, S.A. Halawy. *Thermochim. Acta*, **429**, 57 (2005).
[147] N. Chaiyo, R. Muanghlua, S. Niemcharoen, B. Boonchom, P. Seeharaj, N. Vittayakorn. *J. Therm. Anal. Calorim.*, **107**, 1023 (2012).
[148] E.L. Charsley, S.B. Warrington (Eds.). *Thermal Analysis – Techniques and Applications*, Royal Society of Chemistry, Cambridge (1992).
[149] R. Hocart, N. Gérard, G. Watelle-Marion. *Compt. Rend. Acad., Sci. Paris*, **258**, 3709 (1964).
[150] L. Walter-Levy, J. Laniepce. *Compt. Rend. Acad., Sci. Paris*, **259**, 4685 (1964).
[151] T. Echigo, M. Kimata, A. Kyono, M. Shimizu, T. Hatta. *Mineral. Mag.*, **69**, 77 (2005).
[152] F. Mohandes, F. Davar, M. Salavati-Niasari. *J. Phys. Chem. Solids*, **71**, 1623 (2010).
[153] L. Erdey, S. Gál, G. Liptay. *Talanta*, **11**, 913 (1964).
[154] E.D. Macklen. *J. Inorg. Nucl. Chem.*, **29**, 1229 (1967).
[155] G.C. Nicholson. *J. Inorg. Nucl. Chem.*, **29**, 1599 (1967).
[156] M. Hermanek, R. Zboril, M. Mashlan, L. Machala, O. Schneeweiss. *J. Mater. Chem.*, **16**, 1273 (2006).
[157] P. Hermankova, M. Hermanek, R. Zboril. *Eur. J. Inorg. Chem.*, 1110 (2010).
[158] D. Broadbent, D. Dollimore, J. Dollimore. *J. Chem. Soc. A*, 451 (1967).
[159] B. Małecka, E. Drożdż-Cieśla, A. Małecki. *Thermochim. Acta*, **423**, 13 (2004).
[160] B. Małecka, A. Małecki, E. Drożdż-Cieśla, L. Tortet, P. Llewellyn, F. Rouquerol. *Thermochim. Acta*, **466**, 57 (2007).
[161] I. ul Haq, F. Haider. *J. Chin. Chem. Soc.*, **57**, 343 (2010).
[162] S. Majumdar, I.G. Sharma, A.C. Bidaye, A.K. Suri. *Thermochim. Acta*, **473**, 45 (2008).
[163] B. Donkova, D. Mehandjiev. *Thermochim. Acta*, **421**, 141 (2004).
[164] E. Lamprecht, G.M. Watkins, M.E. Brown. *Thermochim. Acta*, **446**, 91 (2006).
[165] K.P. Pribylov, D.S. Fazluttina. *Russ. J. Inorg. Chem.*, **14**, 344 (1969).
[166] R.I. Frost, A.J. Locke, W.N. Martens. *J. Therm. Anal. Calorim.*, **93**, 993 (2008).
[167] G.E. Delgado, A.J. Mora, E.E. Avila, J. Contreras. *Av. Quím.*, **3**, 43 (2008).
[168] L. Jun, Z. Feng-Xing, R. Yan-Wei, H. Yong-Qian, N. Ye-Fei. *Thermochim. Acta*, **406**, 77 (2003).
[169] A.H. Verdonk. *Thermochim. Acta*, **4**, 25 (1972).
[170] El-H.M. Diefallah, S.N. Basahel, A.A. El-Bellihi. *Thermochim. Acta*, **290**, 123 (1996).
[171] K. Nakamoto. *Infrared and Raman Spectra of Inorganic and Coordination Compounds*, 6th Edn, Wiley, New York (2009).
[172] J. Fujita, A.E. Martell, K. Nakamoto. *J. Chem. Phys.*, **36**, 324 (1962).
[173] J. Fujita, A.E. Martell, K. Nakamoto. *J. Chem. Phys.*, **36**, 331 (1962).
[174] G.M. Begun, W.H. Fletcher. *Spectrochim. Acta*, **19**, 1343 (1963).
[175] T.A. Shippey. *J. Mol. Struct.*, **65**, 61 (1980).
[176] A.R. Hind, S.K. Bhargava, W. Bronswijk, S.C. Grocott, S.L. Eyer. *Appl. Spectrosc.*, **52**, 683 (1998).
[177] R.L. Frost, M.L. Weier. *J. Raman Spectrosc.*, **34**, 776 (2003).
[178] R.L. Frost. *Anal. Chim. Acta*, **517**, 207 (2004).
[179] E.J. Baran. In *Advances in Plant Physiology*, A. Hemantaranjan (Ed.), Vol. 8, pp. 365–392, Scientific Publishers, Jodhpur (2005).
[180] P.V. Monje, E.J. Baran. *Plant Physiol.*, **128**, 707 (2002).
[181] E.L. Varetti, C.R. Volponi. *Appl. Spectrosc.*, **49**, 537 (1995).
[182] H.G.M. Edwards, N.C. Russell, M.R.D. Seaward, D. Slarke. *Spectrochim. Acta, Part A*, **51**, 2091 (1995).
[183] H.G.M. Edwards, M.R.D. Seaward, S.J. Attwood, S.J. Little, L.F.C. de Oliveira, M. Tretiach. *Analyst*, **128**, 1218 (2003).

[184] H.G.M. Edwards, N.C. Russell, M.R.D. Seaward. *Spectrochim. Acta*, **53A**, 99 (1997).
[185] P.V. Monje, E.J. Baran. *Z. Naturforsch.*, **65c**, 429 (2010).
[186] E.J. Baran, C.H. Rolleri. *Rev. Brasil. Bot.*, **33**, 519 (2010).
[187] E.J. Baran, A.C. González-Baró, M.M. Ciciarelli, C.H. Rolleri. *Rev. Biol. Trop.*, **58**, 1507 (2010).
[188] M. Daudon, C. Hennequin, B. Lacour, G. Moel, R. Donsimoni, S. Fellahi, M. Paris, S. Troupel. *Urol. Res.*, **23**, 319 (1995).
[189] L. Estepa, M. Daudon. *Biospectroscopy*, **3**, 347 (1997).
[190] S.K.H. Khalil, M.A. Azooz. *J. Appl. Sci. Res.*, **3**, 387 (2007).
[191] J.R. Guerra-López, J.A. Güida, C.O. Della Védova, R.R. García. *Acta Bioquím. Clín. Latinoamer.*, **42**, 189 (2008).
[192] J.R. Guerra-López, J.A. Güida, C.O. Della Védova. *Urol. Res.*, **38**, 383 (2010).
[193] M.H. Khaskheli, S.T.H. Serráis, U.M. Ujan, S.A. Mahesar. *Turk. J. Chem.*, **36**, 477 (2012).
[194] R. Selvaraju, A. Raja, G. Thiruppathi. *Spectrochim. Acta, Part A*, **99**, 205 (2012).
[195] T.A. Shippey. *J. Mol. Struct.*, **67**, 223 (1980).
[196] M. Cadene, A. Fournel. *J. Mol. Struct.*, **37**, 35 (1977).
[197] R.J.H. Clark, S. Firth. *Spectrochim. Acta, Part A*, **58**, 1731 (2002).
[198] I. Petrov, B. Šoptrajanov. *Spectrochim. Acta, Part A*, **31**, 309 (1975).
[199] T.A. Shippey. *J. Mol. Struct.*, **63**, 157 (1980).
[200] C.G. Kontoyannis, N.C. Bouropoulos, P.G. Koutsoukos. *Appl. Spectrosc.*, **51**, 64 (1997).
[201] D. Valarmathi, L. Abraham, S. Gunasekaran. *Indian J. Pure Appl. Phys.*, **48**, 36 (2010).
[202] M.C. D'Antonio, Nancy Mancilla, A. Wladimirsky, D. Palacios, A.C. González-Baró, E.J. Baran. *Vib. Spectrosc.*, **53**, 218 (2010).
[203] N. Mancilla, V. Caliva, M.C. D'Antonio, A.C. González-Baró, E.J. Baran. *J. Raman Spectrosc.*, **40**, 915 (2009).
[204] A. Wladimirsky, D. Palacios, M.C. D'Antonio, A.C. González-Baró, E.J. Baran. *J. Argent. Chem. Soc.*, **98**, 71 (2011).
[205] M.C. D'Antonio, D. Palacios, L. Coggiola, E.J. Baran. *Spectrochim. Acta, Part A*, **68**, 424 (2007).
[206] R.L. Frost, A. Locke, W.W. Martens. *J. Raman Spectrosc.*, **39**, 901 (2008).
[207] D. Palacios, A. Wladimirsky, M.C. D'Antonio, A.C. González-Baró, E.J. Baran. *Spectrochim. Acta, Part A*, **79**, 1145 (2011).
[208] W.W. Porterfield. *Inorganic Chemistry. A Unified Approach*, 2nd Edn, Academic Press, San Diego, CA (1993).
[209] J.P. Fackler Jr, F.A. Cotton, D.W. Barnum. *Inorg. Chem.*, **2**, 97 (1963).
[210] F.A. Cotton, J.J. Wise. *Inorg. Chem.*, **6**, 917 (1967).
[211] O. Kahn. *Molecular Magnetism*., VCH-Publishers, New York (1993).
[212] I. Sledzinska, A. Murasik, P. Fischer. *J. Phys. C: Solid State Phys.*, **20**, 2247 (1987).
[213] I. Śledzińska, A. Murasik, M. Piotrowski. *Physica B*, **138**, 315 (1986).
[214] S. De, S. Barros, S.A. Friedberg. *Phys. Rev.*, **141**, 637 (1966).
[215] I. Sledzinska, A. Murasik, P. Fischer. *J. Phys. C: Solid State Phys.*, **21**, 5273 (1988).
[216] J.A. Lukin, S. Simizu, N.S. VanderVen, S.A. Friedberg. *J. Magn. Magn. Mater.*, **140–144**, 1669 (1995).
[217] E. Romero, M.E. Mendoza, R. Escudero. *Phys. Status Solidi B*, **248**, 1519 (2011).
[218] S. Vaidya, P. Rastogi, S. Agarwal, S.K. Gupta, T. Ahmad, A.M. Antonelli, K.V. Ramanujachary, S.E. Lofland, A.K. Ganguli. *J. Phys. Chem. C*, **112**, 12610 (2008).
[219] E. Romero-Tela, M.E. Mendoza, R. Escudero. *J. Phys. Condens. Matter*, **24**, 196003 (2012).
[220] L. Dubicki, C.M. Harris, E. Kokot, R.L. Martin. *Inorg. Chem.*, **5**, 93 (1966).
[221] J.J. Girerd, O. Kahn, M. Verdaguer. *Inorg. Chem.*, **19**, 274 (1980).
[222] K.T. McGregor, Z.G. Soos. *Inorg. Chem.*, **15**, 2159 (1976).
[223] D.Y. Jeter, W.F. Hatfield. *Inorg. Chim. Acta*, **6**, 523 (1972).
[224] G. Delgado, A.J. Mora, V. Sagredo. *Physica B*, **320**, 410 (2002).
[225] M. Gerloch, J. Lewis, R.C. Slade. *J. Chem. Soc. A*, 1422 (1969).
[226] D. Collison, A.K. Powell. *Inorg. Chem.*, **29**, 4735 (1990).
[227] E. Fluck, W. Kerler, W. Neuwirth. *Angew. Chem.*, **75**, 461 (1963).
[228] F. Aramu, V. Maxia, C. Muntoni. *Hyperfine Interact.*, **5**, 399 (1978).
[229] J.T. Wrobleski, D.R. Brown. *Inorg. Chem.*, **18**, 2738 (1979).
[230] A. Abras, E. Figueiredo de Oliveira. *Hyperfine Interact.*, **66**, 271 (1991).
[231] J.V. De Menezes, F. de S. Barros. *Phys. Status Solidi A*, **45**, K139 (1978).
[232] G.M. Bancroft, K.G. Dharmawardena, A.G. Maddock. *Inorg. Chem.*, **9**, 223 (1970).
[233] H. Sato, T. Tominaga. *Bull. Chem. Soc. Jpn.*, **52**, 1402 (1979).
[234] J. Ladriere. *Hyperfine Interact.*, **70**, 1095 (1992).